2011

AN ALTERNATIVE TO CHROMATES FOR CORROSION PROTECTION FOR ALUMINUM ALLOYS

Melissa Williams
University of Rhode Island, mwilliams@my.uri.edu

AN ALTERNATIVE TO CHROMATES FOR CORROSION PROTECTION FOR ALUMINUM ALLOYS

BY

MELISSA WILLIAMS

A THESIS SUBMITTED IN PARTIAL FULFILLMENT OF THE REQUIREMENTS FOR THE DEGREE OF

MASTER OF SCIENCE

IN

CHEMICAL ENGINEERING

UNIVERSITY OF RHODE ISLAND

2011

MASTER OF SCIENCE THESIS

OF

MELISSA WILLIAMS

APPROVED:

Thesis Committee:

Major Professor Richard Brown

Geoffrey Bothun

Sze Yang

Nasser H. Zawia
DEAN OF THE GRADUATE SCHOOL

UNIVERSITY OF RHODE ISLAND
2011

ABSTRACT

Aluminum alloys, such as Al 6061-T6 and Al 7075-T6, are widely used in industry due to their high strength to weight ratio and good mechanical properties. The corrosion of these alloys, however, is an expensive and critical problem since the alloys are susceptible to pitting and crevice corrosion in marine environments. The most significant environmental factor, which contributes to the corrosion of these alloys, is the chloride ion found in marine environments or water condensed from humid air contaminated with soluble chloride salts.

Traditionally, chromate based conversion coatings have been used for many years for the protection of aluminum alloys. Chromates are efficient corrosion inhibitors for aluminum and its alloys in near neutral marine environments containing aggressive anions such as chlorides. Although the hexavalent chromium ion, Cr^{6+}, may be a superior corrosion inhibitor and used in numerous industrial systems, it is environmentally unsafe. Over the past several years, federal agencies, such as the Environmental Protection Agency (EPA) and the Department of Defense (DoD), have increasingly limited the use of chromium containing compounds due to their toxic and carcinogenic effects. In addition, there is a direct economic challenge associated with costs for environmental compliance along with increased liability for claims of exposure in the workplace with the continued use of chromates. Therefore, there is a need to identify new corrosion inhibitors for aluminum alloys.

As an alternate conversion coating, a new titanate conversion coating was researched and developed for the Al 2024-T3 alloy and was shown to be effective. The

objective of this research was to determine if the coating process could be applied to Al 6061-T6 and Al 7075-T6. The coating process involves immersion of the alloy in a titante solution bath, which produces a passive film. The corrosion resistance of coated samples has been evaluated using electrochemical impedance spectroscopy (EIS) and potentiodynamic electrochemical techniques. Electrochemical testing and energy dispersive X-ray analysis indicated that the titanate ion would retard corrosion in a similar manner to the chromate ion if fluoride ions (F^-) were not present on the surface.

A study was also conducted to determine if Al 6061-T6 and Al 7075-T6 were easily susceptible to crevice corrosion in a marine environment. The study yielded important results regarding protection of the alloy against crevice corrosion by the titanate ion. Corrosion was only seen on samples not exposed to the titanate ion. A conclusion may be made that titanate coatings appear to be viable alternatives to chromate coatings but further investigation will be required in order to determine an optimum conversion coating bath, which will produce impedance magnitudes comparable to those measured for the Al 2024-T3 alloy.

ACKNOWLEDGMENTS

I would first like to sincerely thank my major professor, Dr. Richard Brown, for his wisdom, guidance and encouragement. Working for him for the past two years has been an amazing experience. He has taught me how to look behind the surface and has helped me to grow as a student and an engineer. I would also like to thank Dr. Geoffrey Bothun and Dr. Sze Yang for serving on my thesis committee as well as Dr. Leon Thiem for acting as my defense chair.

I would also like to take this opportunity to thank Dr. Stanley Barnett for his immense wealth of knowledge and his guidance throughout both my undergraduate and graduate studies. Thank you for always having a joke on hand to ease my stress.

I also want to thank Brenda Moyer and Mary Strawderman for always being there for me. I can't count the number of times I've gone to the office just to sit and talk and you were both always there to listen and give advice. I will truly miss you both.

I would like to thank two of my closest friends who have been there through the good times and some of the worst times, Michelle and Alex. Michelle, this past year in Crawford has not been the same without you. Thank you from the bottom of my heart for your friendship. You will always have a place to come home to. Alex, you may live far away now but you've always been there when I needed you and I thank you for that. Your friendship means the world to me.

I also would like to thank my second families, the Sibielski family and the Ellis family. Leon and Shirl, thanks for always looking out for me and loving me. Ben and Becky, your friendships mean everything to me. Thank you both for always being there. Aunty Karen and Uncle Ted, it's hard to find the words to say thank you for all you have done for me and to tell you how much you mean to me. Katie, the word "sister" doesn't begin to describe our relationship. I will always be here for you like you have been for me. Thank you for everything.

I would like to give my most sincere thanks to my family who has always been there. Uncle Mitchell, Aunty Sandy, Jeremy, Matthew and Marcy, your love and support mean the world to me. Thank you for always believing in me. Jeremy and Matthew, thank you for looking out for me and being the big brothers I never had. Jeremy, thanks for inspiring me to become a chemical engineer.

Finally, I would like to give my most heartfelt and bottomless thanks to the people who mean the most to me. Mom and Dad, words can't begin to describe how thankful I am for the two of you. Thank you for always believing in me and supporting me. You are my anchors. I love you.

Brian, thank you for your love and your support. I can't wait to figure it all out with you. Beijos.

Bubby, this is for you. It's always for you.

TABLE OF CONTENTS

CHAPTER III – EXPERIMENTAL RESULTS

CHAPTER IV – DISCUSSION

LIST OF TABLES

CHAPTER I

CHAPTER II

CHAPTER IV

LIST OF FIGURES

CHAPTER I

CHAPTER II

CHAPTER III

CHAPTER IV

CHAPTER I

INTRODUCTION

1.1 Microstructure of Al 6061-T6 and Al 7075-T6

Aluminum (Al), when coupled with small amounts of other materials, is a fundamental and beneficial metal used in a wide range of industrial applications due to its high specific strength [1]. These alloys are commonly used in marine applications where low-density materials, good mechanical properties and improved resistance to corrosion are desired [2]. Aluminum alloy 6061-T6 is known for its superior mechanical properties, such as high strength to weight ratio, good ductility and good corrosion resistance [3]. The composition of this alloy is 1.0% Mg and 0.6% Si and lesser amounts of Cu, Mn, Fe and Cr. The balance of the alloy is aluminum. Aluminum alloy 7075-T6 is extensively used for structural applications due to its high strength/density ratio and reasonable high fracture toughness [4]. The composition of this alloy is 5.5% Zn, 2.6% Mg, 1.55% Cu and lesser amounts of Cr, Si, Mn and Fe. Once again, the balance of the alloy is aluminum. The "T6" classification indicates that the alloy was solution treated and artificially aged [5].

During solidification and thermomechanical processing, heterogeneous microstructures are developed to produce a desirable mix of mechanical properties. The dominant feature of alloy microstructures is the distribution of second-phase particles that contain high concentrations of alloying and impurity elements [6]. These particles have electrochemical characteristics that differ from the surrounding alloy matrix, making the alloy more susceptible, in general, to localized corrosion.

The predominant second phases present in Al 6061-T6 are Al-Mg-Si particles. Mg and Si combine together to form very stable Mg_2Si and commercial alloys are based on the pseudo binary system of Al-Mg_2Si. The predominant second phases present in Al 7075-T6 are Zn-Mg-Cu particles, where Zn and Mg merge together to form $MgZn_2$.

1.2 Corrosion of Al 6061-T6 and Al 7075-T6

Corrosion, in general, can be defined as the "degradation of engineering materials by exposure to a wet surface [7]." For corrosion of a metal to take place, four conditions need to be satisfied. The first process is an oxidation or anodic reaction. The second is a reduction or cathodic reaction and the third is ionic transport for which a conductive electrolyte is required, such as water, seawater, or an acidic or basic solution. Finally, the fourth process is electron transport between the anode and cathode. If one of these processes is not present, corrosion will not occur.

If these alloys are left untreated, they will corrode at a rate depending on the alloys composition and local environment. Generally, aluminum is resistant to most environments due to a layer of oxide film, which forms on the surface and reforms rapidly if damaged. However, this film is an insufficient barrier for relatively long-term corrosion protection. This is because aluminum is able to react both as a base or an acid, which means its oxide film is stable in neutral conditions but soluble in acidic and alkaline environments. This relationship is expressed by the Pourbaix diagram, which shows the relationship between potential and the solution pH. Figure 1-1 is the

Pourbaix diagram for aluminum, which indicates the circumstances in which aluminum should show corrosion [8].

The resistance of aluminum to corrosion depends significantly on its purity and microstructure. Pure aluminum is more resistant than any of its alloys. The 6xxx series alloys are susceptible to corrosion but resistance decreases as the copper and iron content increase. At copper levels higher than 0.5%, intergranular corrosion can occur. Also, when the magnesium and silicon contents in Al 6061 are balanced to form only Mg_2Si, corrosion is slight, but if the alloy contains silicon in excess of that needed to form Mg_2Si, susceptibility to corrosion increases. Al 7075, which contains a significant amount of copper, is less resistant to corrosion than those of the same series that do not contain copper, as well as the 6xxx series.

The most common form of aluminum corrosion is pitting, which is a localized corrosion form. It has been attributed to the breakdown of the natural passive film on the metal. The resistance to pitting corrosion is then determined by the electrochemical stability of the protective passive film. The tendency for pitting for a given metal-electrolyte system is defined by the pitting potential (E_p), which is the potential above which pits will initiate and below which they will not [9]. For aluminum, pitting corrosion is most commonly produced by halide ions, of which the chloride (Cl^-) is the most frequently found. The presence of chlorides can create local corrosion potential drops between the metal surface and the obstructed region at which the chloride is accumulated. Chlorides facilitate the breakdown of the oxide film by forming $AlCl_3$. When aluminum ions migrate away from the pits, alumina precipitates as a membrane, which further isolates local acidity and pitting of the metal results [8].

Pitting can be separated into two different stages, namely pit initiation and pit growth. While the growth mechanism is well understood, the initiation mechanism is not very clear. However, pitting has been shown to initiate at constituent particles, which are either anodic or cathodic relative to the matrix. Local interactions between the particles and the matrix enhance the rate of pit growth. In Al 7075-T6 samples, the constituent particles show significant pitting after being exposed to sodium chloride (NaCl) solution. It can also be seen that pits developed around neighboring constituent particles tend to coalesce to form larger pits. Research has been done, which presents standard electrode potentials of the strengthening precipitates as well as constituent particles. The Mg_2Si particles found in Al 6061-T6 and the $MgZn_2$ particles found in Al 7075-T6 are both significantly anodic. The presence of anodic particles implies that they contribute to the overall pitting process after long exposures to NaCl [10].

Once initiation takes place, pits begin to increase in size. The exposed surface outside the growing pit is cathodically protected by the reduction of oxygen to hydroxyl ion (OH^-) reaction:

$$O_2 + 2H_2O + 4e^- \rightarrow 4OH^- \text{ (reduction half cell reaction)} \quad (1)$$

As this cathodically protects the region outside the pit, the metal dissolution region cannot spread laterally across the surface. In addition, the large cathodic surface can maintain this reaction and form a large cathode to small anode ratio, which accelerates the anodic reaction. Within the pit, the metal dissolution reaction is taking place. This is the anodic reaction of:

$$Al \rightarrow Al^{3+} + 3e^- \text{ (oxidation half cell reaction)} \quad (2)$$

Since it is the only reaction within the pit, an electrical imbalance results again, thereby attracting negatively charged ions, usually chloride ions. The autocatalytic reaction to form hydrochloric acid in the pit is initiated and continues:

$$AlCl_3 + 3H_2O \rightarrow Al(OH)_3 + 3HCl \quad (3)$$

Since pitting is an autocatalytic reaction, once it is started, the pH decreases while the chloride ion concentration increases inside the pit. The pitting mechanism can be seen in Figure 1-2 for both Al 6061 and Al 7075 alloys.

One other type of possible corrosion that may be seen on aluminum alloys is crevice corrosion. The general conditions include a stagnant solution and a gap between two surfaces, one of which is metal. Initially, the usual cathodic (Eqn 1) and anodic (Eqn 2) reactions occur over the surface of the metal. However, a restriction occurs in the crevice region in which the dissolved oxygen in the crevice cannot easily be replaced. Therefore, the region inside the crevice cannot support a cathodic reaction but can still support an anodic reaction. Outside the crevice region the cathodic reaction proceeds but the anodic reaction ceases.

An electrical charge imbalance exists between the high positive charge from the metal ions within the crevice and the negative charge outside the crevice. As a result, negative ions, such as chloride ions, are attracted into the crevice. Associated with the negative chloride ion is the positive hydrogen ion. Both the chloride ion concentration and the hydrogen ion concentration increase within the crevice, decreasing the pH to acidic conditions, which allows the corrosion rate inside the crevice to increase. This mechanism can be seen in Figure 1-3 [11].

1.3 Corrosion Protection of Al 6061-T6 and Al 7075-T6

The most significant environmental factor, which contributes to the corrosion of these alloys, is the chloride ion found in marine environments or water condensed from humid air contaminated with soluble chloride salts [12]. Since long-term corrosion resistance is unlikely due to the thin natural oxide film, a finishing process is required to reduce corrosion susceptibility. To prevent rapid deterioration, various methods, which usually involve several layers of protection on top of the Al substrate, have been developed. For example, an artificially thick aluminum oxide (Al_2O_3) layer can be grown, either chemically or electrochemically, directly above the bare alloy. This allows for various paints and coatings to be applied to the oxide film.

Corrosion resistant coatings prevent corrosion on aluminum alloys by various methods, including barrier protection and active corrosion protection as well as conversion coatings. Barrier coatings prevent contact of the underlying aluminum substrate with the environment. They are either organic or inorganic and work to suppress the cathodic reaction and limit the transport of electrons to the metal surface. In the active corrosion protection strategy, corrosion inhibitors are used to slow the corrosion cell process on aluminum by undergoing reduction at the active corrosion sites to form insoluble oxides. This provides a barrier against corrosion by limiting the permeability of electrolytes, such as chloride ions.

Conversion coatings are applied to aluminum and aluminum alloys to improve corrosion resistance or to improve adhesion. It is a term that describes the removal of the native oxide on a metal and its replacement with an oxide coating that provides a barrier to corrosion. Conversion coatings are adherent surface layers of low-solubility

oxide phosphate or chromate compounds produced by the reaction of suitable reagents with the metallic surface. These coatings affect the appearance, electrochemical potential, electrical resistivity, surface hardness, absorption, and other surface properties of the material. They are formed by a chemical oxidation-reduction reaction at the surface of the aluminum [13]. Currently, the most effective and widely used way to inhibit corrosion of aluminum alloys is a chromate-based conversion coating.

1.4 Corrosion Inhibition by Chromates

Cr(VI) compounds, mainly chromates, are widely used as corrosion inhibitors in aqueous media. A wide range of metals and alloys, such as iron, steel, aluminum alloys, zinc, copper, and others, can be protected using chromates. Their high efficiency to cost ratio has made them the standard inhibitors [14].

There are many ways to inhibit corrosion through the use of Cr(VI) compounds. Two of the most prominent are chromic acid anodization and chromate conversion coatings. Chromic acid anodization involves the electrochemical growth of an aluminum oxide surface film in an aqueous solution where a non-porous oxide layer is formed with a thicker porous layer above it. Coatings on aluminum alloys are on the order of 2-50 μm in thickness. Anodization is carried out in an acidic bath, which contains ingredients that promote formation of an adherent oxide film [15]. Chromates seal the porous layer with chromic acid (H_2CrO_4), producing a thicker oxide layer, which provides barrier protection for the bare metal as well as providing active passivation. Although anodization offers superior corrosion protection, chromate conversion coatings are more preferable due to economic benefits and

practicality. Anodization can be expensive and therefore not affordable when dealing with large aluminum structures.

Chromate conversion coatings are generally used to increase the corrosion resistance of aluminum. The high corrosion resistance provided by chromate coatings is due to the presence of hexavalent and trivalent chromium ions. The trivalent chromium, Cr^{3+} or Cr(III), is present as an insoluble hydrated oxide, while the hexavalent chromium, Cr^{6+} or Cr(VI), adds a self-healing nature to the film during corrosive attack by species such as chloride ions. During corrosion, the hexavalent chromium is reduced to form trivalent chromium, which terminates the corrosive attack [13].

Chromate ions increase the pitting potential of aluminum alloys in chloride media and inhibit pit initiation and dissolution of active intermetallic phases. Chromate conversion coatings (CCC) form on aluminum through reduction of Cr^{6+} (dichromate) in solution and are usually acidic with a pH between the range of 1.6 and 3.0. Coating formation is assisted by the addition of sodium fluoride (NaF), which helps to activate the aluminum surface. A CCC is a chemically grown oxide layer on the alloy substrate that provides an active barrier layer, which reduces the rate of the cathodic oxygen reaction. The chemical and electronic variety found in Cr chemistry leads to the ability of Cr^{6+} oxoanions to inhibit corrosion [16]. The electrochemical reactions for the chromate conversion coating process are well known [17].

$$Cr_2O_7^{2-} + 8H^+ + 6e^- \rightarrow 2Cr(OH)_3 + H_2O \quad (4)$$

$$2Al \rightarrow 2Al^{3+} + 6e^- \quad (5)$$

Understanding the mechanism for chromate inhibition of aluminum alloy dissolution is important. Chromate is a very soluble and a high-valent oxidizing ion with a low-valent form that is insoluble. The oxidation of Al in the presence of competing fluoride ions produces electrons to reduce the hexavalent Cr^{6+} of the dichromate ion, $Cr_2O_7^{2-}$ and form a protective hydrated 3-valent $Cr(OH_{3)}$. The final result is a film thickness of at least several hundred nanometers on matrix regions, with thinner coatings at second phase particles [18]. This film, which provides the barrier protection against corrosion, is one mechanism of corrosion protection offered by CCCs.

Another very important mechanism is the self-healing feature of chromate conversion coatings. The coating layer consists of an amorphous and insoluble chromium oxide, where the formation of Cr(III)-O-Cr(VI) bonds takes place. These bonds act as adsorption sites for chromate ions from the coating bath. Therefore, the coating is a mixture of hydrated amorphous Cr(III)-Cr(VI) oxide. Where Cr(VI) is in contact with the electrolyte, it migrates to the defects of the coating layer, where it is more susceptible to corrosion attack [19]. In other words, the easily broken down hexavalent chromium in the coating is released into a solution contacting the surface. Chromate ions are released by the coating, and can be transferred to the site of damage to help repair the film by reduction of the chromate to a chromic species that bond with the aluminum substrate and the existing coating [20]. This self-healing aspect, which includes the transportation of Cr(VI) species to an active corrosion site and the subsequent blocking of corrosion sites, is a main reason chromate films are so effective.

Chromate conversion coatings are artificially thick, chemically grown oxide layers on the Al surface (military specifications MIL-C-81706/5541E). They have been shown to consist of particles ranging in size from ~ 10 nm to 60 nm. There are three distinct regions in the chromate conversion coating that have been observed: (1) a region lacking particles but containing Cr or Al, (2) a region throughout the film largely containing particles of Cr compounds, and (3) particles near the base of the film with Cr and Al. Past studies observed crystallographic orientations of the Al substrate and found hydrated chromium oxide ($Cr_2O_3 \cdot H_2O$) was deposited at cathodic sites or grain boundaries near metal ridges on the Al surface. The anodic sites were between the metal ridges, where Al was dissolved. Other research indicated amorphous Cr(III) hydroxide ($Cr(OH)_3$) or Cr(III) oxide (Cr_2O_3) within the film, but Cr(VI) only at the surface [1].

It has been proposed that three factors contribute to the performance of chromate conversion coatings: (1) barrier protection, (2) hydrophobicity and (3) active species that protect weak spots or emerging pits. The oxide layer itself is inert and acts as a barrier layer, which provides protection to the underlying bare metal. Although it is a clear fact that Cr(VI) is the active species in chromate conversion coatings, where corrosion protection is provided by the reduction of Cr^{6+} to Cr^{3+}, precisely how chromate works to forestall corrosion remains unclear. In addition, in spite of its good performance as an anti-corrosion treatment, the Cr(VI) species are well known to be environmentally unfriendly.

1.5 Toxicity of Chromates

Studies over the past 10-15 years indicate that chromates are both highly toxic and carcinogenic. The oral ingestion of chromates is known to cause gastrointestinal damage, kidney failure, liver damage, blood disorders and eventually death. Prolonged exposure to skin may cause rashes, blisters, and ulcers and has also been associated with lung cancer and intestinal tumors. Chromates can also penetrate the body by inhalation, which may eventually cause lung cancer.

Although Cr^{6+} may be a superior corrosion inhibitor and used in numerous industrial systems, the same properties that make it so are also the same that make it environmentally unsafe. Earlier studies document Cr(VI) as a human carcinogenic associated with lung cancer. However, it is not the static presence of Cr^{3+} or Cr^{6+} that contributes directly to the DNA damage that leads to cancer. Rather, the molecular debris associated with the process of reducing Cr^{6+} to Cr^{3+} induces the critical changes in DNA. Chromate alone does not damage DNA in the absence of reducing agents. Instead, it is the biological antioxidants that lead to DNA damage.

The intracellular reaction of Cr^{6+} in the presence of reducing agents produces Cr^{5+}, Cr^{4+}, Cr^{3+}, free radicals and reactive oxygen, which are all potentially genotoxic. Although there is no general agreement on the details for Cr^{6+}-induced damage to DNA, it is clear that Cr^{6+} is highly soluble in water and passes through cell membranes. In addition, small molecule antioxidants appear to form highly reactive intermediates such as Cr^{5+} and Cr^{4+}, which in turn react either directly or through free radical intermediates to damage DNA [16].

1.6 Alternatives to Chromate Conversion Coatings

Due to the highly toxic and carcinogenic nature of Cr(VI), and it being far from environmentally friendly, research studies have begun to focus greater attention on non-Cr(VI) conversion processes. Low toxicity conversion coatings prepared in non-Cr(VI) solutions, such as titanium, zirconium, molybdenum and cerium salt baths, have been widely researched and developed. Although they have the potential to replace existing Cr(VI) conversion coatings, their anticorrosive performance remains inferior.

In recent years, studies have been done to find more ecological alternatives to protecting aluminum alloy surfaces in order to replace chromates in their different fields of application. Efforts have been focused on the search for new corrosion inhibitors and new formulations of both anodizing baths and conversion coatings. However, many of the new systems are still in the beginning stages and many alternative technologies are being investigated.

In the last five to six years, researchers have begun to look at trivalent chromium conversion coatings as a promising alternative because their treatment solutions are less toxic than hexavalent compounds but seem to produce similar results. However, the Cr(III) conversion process is a novel study for aluminum alloys [21].

Other possible replacement technologies that have received considerable attention in the open literature and/or have reached the trial stages in various aluminum industries include organic-based conversion coatings, multivalent metals conversion coatings and lithium-inhibited hydrotalcite conversion coatings. Table 1-1 lists a number of experimental and developmental technologies that can lead to

breakthroughs with respect to replacement of chromium in conversion coatings in some applications [22].

1.7 Significance of Study

Chromates have been around since the early 1900s as a means to control the corrosion of active metals. However, over the past several years the Environmental Protection Agency (EPA) has increasingly limited the use of chromium containing compounds due to their toxic and carcinogenic effects. The EPA is the main regulator of chromate uses and emissions through several different acts, including the Clean Air Act, the Clean Water Act, the Comprehensive Environmental Response, Compensation and Liability Act (CRCLA) and the Toxic Substances Control Act (TSCA). In the 1990s, national emission standards for hazardous air pollutants (NESHAP) were proposed for chromium in the Clean Air Act. In 2009, the Department of Defense (DoD) sent out an aggressive memorandum directing Military Departments to research and develop substitutes to the use of Cr^{6+} [23].

Restrictions and environmental burdens of using chromates are always increasing. Environmentally, industry must comply with lower limits of exposure to workers along with controlled release and cleanup of byproducts and waste generated by its use. In 2006, the permissible exposure limit (PEL) of Cr^{6+} was 52 $\mu g/m^3$. As of 2008, the Occupational Safety and Health Administration (OSHA) established an 8-hour time-weighted average (TWA) exposure limit of 5 $\mu g/m^3$ [24]. Besides environmental issues, there is also an economic burden of using chromates. There is a direct economic challenge associated with costs for environmental compliance along

with increased liability for claims of exposure in the workplace with the continued use of chromates. Therefore, there is a need to identify new corrosion inhibitors for aluminum alloys.

A new approach is to replace the chromate ion with the titanate ion since titanium is an element that has many similarities to chromium. It is one of the elements whose Pourbaix diagram closely resembles that of chromium. Pourbaix diagrams show the relationship between potential and the solution pH to predict whether an electrode will be immune, active or passive in the environment [25]. Figure 1-4 and Figure 1-5 are the Pourbaix diagrams for titanium and chromium, respectively [26]. Titanium is immune to corrosion in all-natural environments. The good corrosion resistance of titanium is due to the formation of a highly stable, continuous, very adherent and protective oxide film on the metal surface. The main similarities between titanium based solutions and that of chromium are that they have multiple valence states, good passive layer formation and a low passivation potential.

For Al 2024-T3, titanate replacement of chromate has shown to be effective [27]. It was found that coating formation was pH dependent, with a pH of 2 resulting in thick coatings but severe cracking. A pH of 5.5 was found to produce coherent coating with good corrosion resistance. The titanate coating on Al 2024-T3 covered the copper rich intermetallics as well as the aluminum matrix, so it could act as a cathodic inhibitor on the cathodic particles as well as an anodic inhibitor on the aluminum particles [28]. Other than Al 2024, there has been little to no work conducted on other aluminum alloys of industrial interest, such as Al 6061 and Al 7075.

The objectives of the research are:

1. To determine if the titanate coating process, successfully utilized on Al 2024-T3, can be applied to Al 6061-T6 and Al 7075-T6.

2. To investigate the basic mechanisms of coating formation, such as the coating composition and deposition rates along with mechanisms of corrosion protection.

Process Description	Status
Trivalent chromium conversion coatings	• Meets no corrosion in 500 h requirement (ASTM B 117 salt spray test) • Still contains chromium • Electrolytic process
Hydrated alumina coating	• Poor paint adhesion • Meets no corrosion in 500 h requirement (ASTM B 117 salt spray test)
Hydrated Metal salt coating (Mg, Ni, Mn, Sn, Ti, Fe, Co, Ca, Ba)	• Does not meet salt spray requirement • Poor adhesion
Peroxide Oxidation Coating	• Does not meet salt spray requirement, poor adhesion and unstable chemical baths
Oxyanion analogs (molybdnates, tungstates, vanadates and permanganates)	• Moderate corrosion resistance, poor paint adhesion • Expensive
Potassium permanganate coatings	• Moderate corrosion protection (168 h) • Poor wet tape adhesion • Does not work well on 2024 or 7075 • Multistep process, expensive
Rare earth metal salts (Cerium)	• Corrosion protection close to that of chromium • Good paint adhesion • Unstable chemical bath and expensive
Zirconium Oxide/yttrium oxide in aqueous polymeric solution	• Good paint adhesion and moderate salt spray protection (100 h) • Commercially used for >10 yr • One step • Expensive
Titanates	• Good adhesion • Moderate corrosion resistance • Thickness dependent, must be cured and difficult to dispose of
Lithium inhibited hydrotalcite coatings	• Good corrosion protection of 6000- series aluminum alloys • Poor wet paint adhesion • Single process bath • Environmentally benign

Table 1-1: Alternative conversion coatings to chromates.

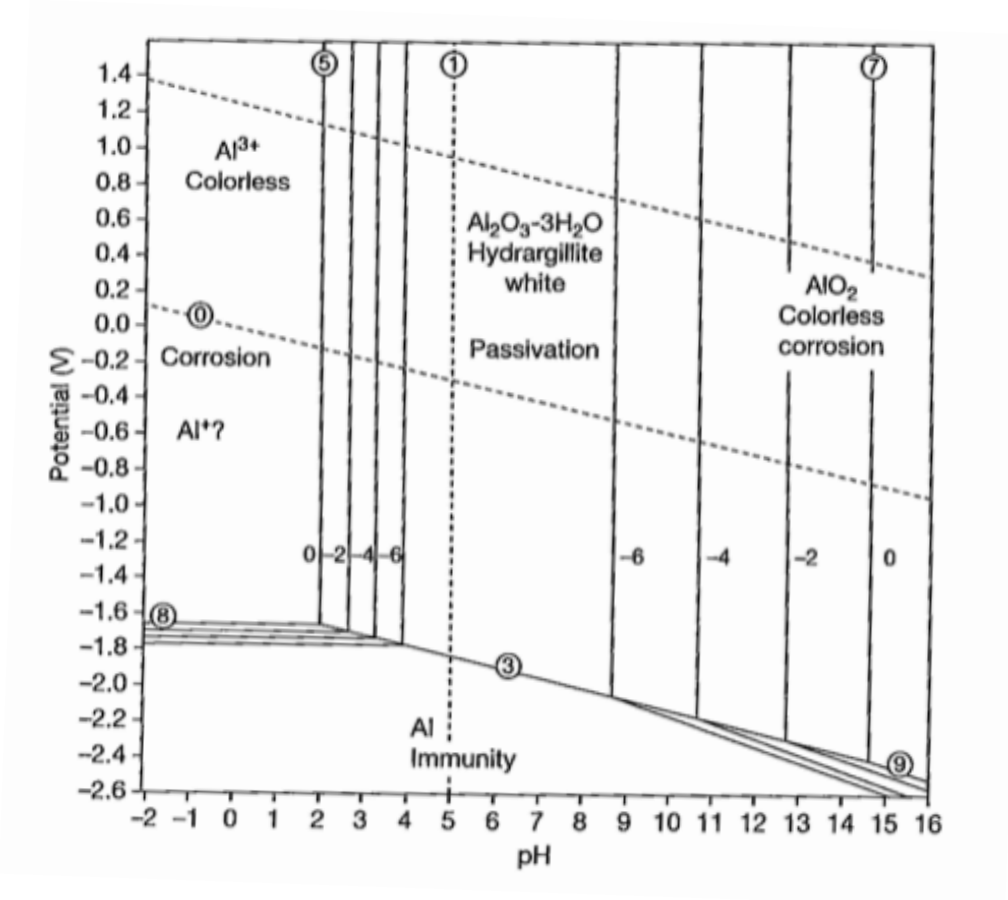

Figure 1-1: Pourbaix diagram for Aluminum.

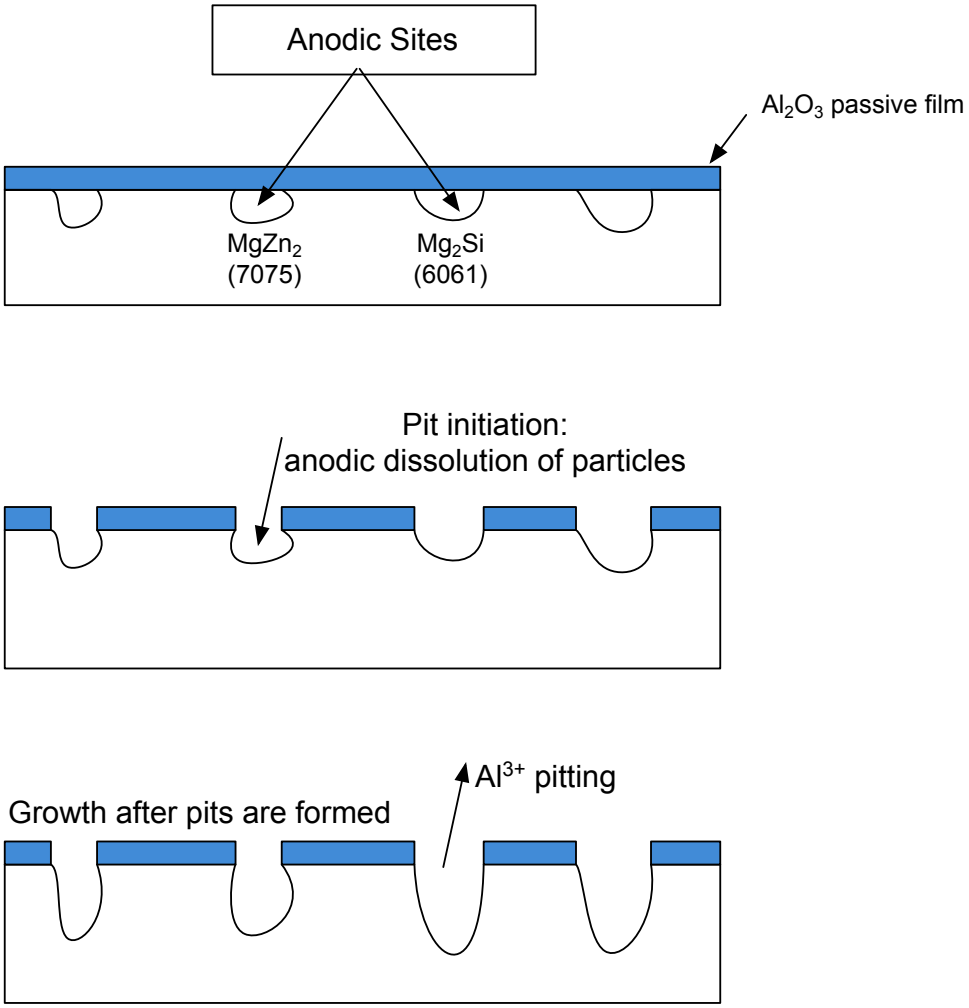

Figure 2-2: Mechanism for pitting corrosion.

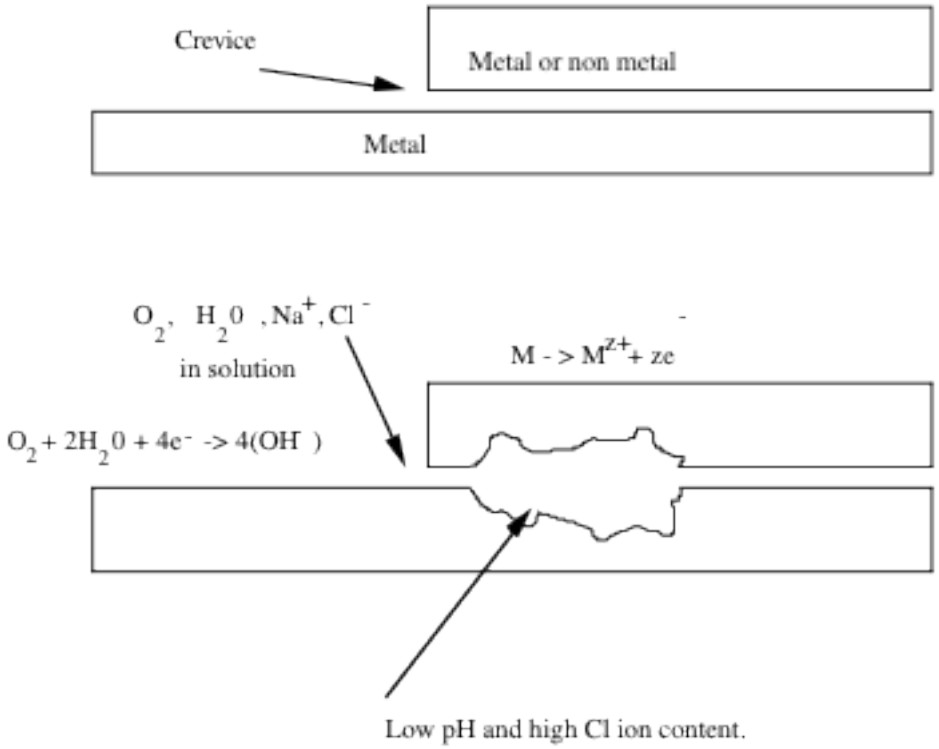

Figure 3-3: Mechanism for crevice corrosion.

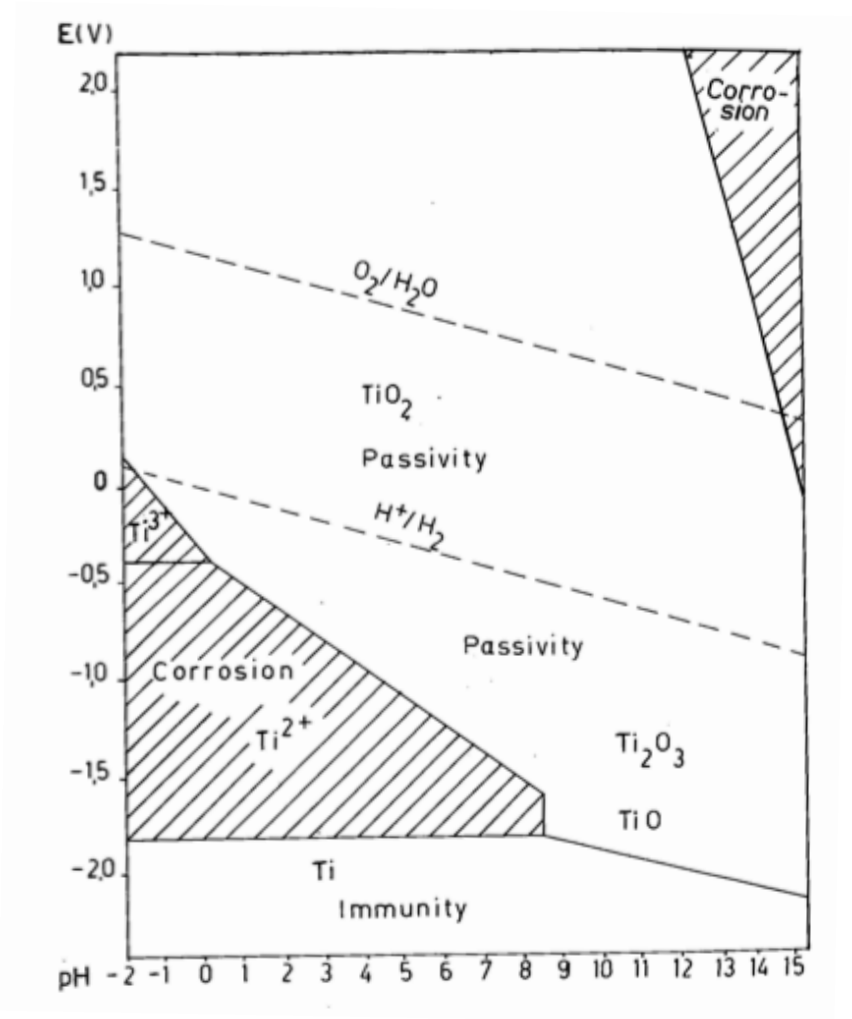

Figure 4-4: Pourbaix diagram for Titanium.

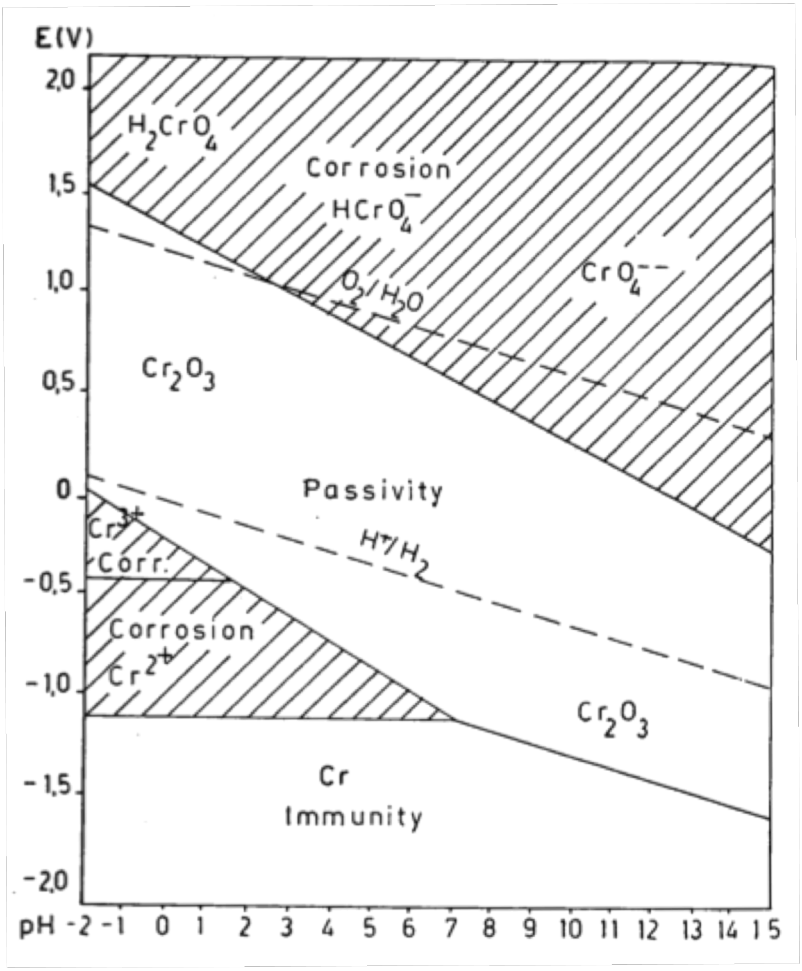

Figure 5-5: Pourbaix diagram for Chromium.

References

1. Cohen, S.M. (1995). Review - Replacements for Chromium Pretreatments on Aluminum. *Corrosion*, 51(1): p. 71-78.

2. Ezuber, H., A. El-Houd, and F. El-Shawesh (2008). A study on the corrosion behavior of aluminum alloys in seawater. *Materials & Design*, 29(4): p. 801-805.

3. Jogi, B.F., et al. (2008). Some studies on fatigue crack growth rate of aluminum alloy 6061. *Journal of Materials Processing Technology*, 201(1-3): p. 380-384.

4. Jayaganthan, R., et al. (2010). Microstructure and texture evolution in cryorolled Al 7075 alloy. *Journal of Alloys and Compounds*, 496(1-2): p. 183-188.

5. Davis, J.R. (1999). Corrosion of Aluminum and Aluminum Alloys, ASM International, p. 267.

6. Buchheit, R.G. (1995). A Compilation of Corrosion Potentials Reported for Intermetallic Phases in Aluminum-Alloys. *Journal of the Electrochemical Society*, 142(11): p. 3994-3996.

7. Brown, R. Chapter 1: Introduction. Retrieved from Lecture Online Web Site: http://www.egr.uri.edu/che/course/CHE534w/CHE534Index.htm, February 8, 2011.

8. Scamans, G.M., N. Birbilis, and R.G. Buchheit (2010). Shreir's Corrosion: Corrosion of Aluminum and its Alloys, p. 1986-1987.

9. Davis, J.R. (1999). Corrosion of Aluminum and Aluminum Alloys, ASM International, p. 30.

10. Dey, S., M.K. Gunjan, and I. Chattoraj (2008). Effect of temper on the distribution of pits in AA7075 alloys. *Corrosion Science*, 50(10): p. 2895-2901.

11. Brown, R. Chapter 5: Localized Corrosion. Retrieved from Lecture Online Web Site: http://www.egr.uri.edu/che/course/CHE534w/CHE534Index.htm, February 10, 2011.

12. Maddala, D. (2007). An Alternate Coating Process for Corrosion Resistance on Aluminum Alloy 2024-T3. MS Thesis, University of Rhode Island, p. 4.

13. Davis, J.R. (1999). Corrosion of Aluminum and Aluminum Alloys, ASM International, p. 206-208.

14. Campestrini, P., et al. (2004). Chromate conversion coating on aluminum alloys - I. Formation mechanism. *Journal of the Electrochemical Society*, 151(2): p. B59-B70.

15. Scamans, G.M., N. Birbilis, and R.G. Buchheit (2010). Shreir's Corrosion: Corrosion of Aluminum and its Alloys, p. 2005.

16. Kendig, M.W. and R.G. Buchheit (2003). Corrosion inhibition of aluminum and aluminum alloys by soluble chromates, chromate coatings, and chromate-free coatings. *Corrosion*, 59(5): p. 379-400.

17. Lunder, O., et al. (2005). Formation and characterisation of a chromate conversion coating on AA6060 aluminium. *Corrosion Science*, 47(7): p. 1604-1624.

18. Liu, Y., et al. (2005). Ageing effects in the growth of chromate conversion coatings on aluminium. *Corrosion Science*, 47(1): p. 145-150.

19. Grilli, R., et al. (2011). Corrosion behaviour of a 2219 aluminum alloy treated with a chromate conversion coating exposed to a 3.5% NaCl solution. *Corrosion Science*, 53(4): p. 1214-1223.

20. Scamans, G.M., N. Birbilis, and R.G. Buchheit (2010). Shreir's Corrosion: Corrosion of Aluminum and its Alloys, p. 2002-2003.

21. Chen, W.K., et al. (2010). The effect of chromic sulfate concentration and immersion time on the structures and anticorrosive performance of the Cr(III) conversion coatings on aluminum alloys. *Applied Surface Science*, 256(16): p. 4924-4929.

22. Davis, J.R. (1999). Corrosion of Aluminum and Aluminum Alloys, ASM International, p. 209.

23. Young, J.J. "Memorandum for Secretaries of the Military Departments: Minimizing the Use of Hexavalent Chromium (Cr6+)", Department of Defense, April 8, 2009.

24. OSHA. "Hexavalent Chromium", Occupational Safety and Health Administration, 2009.

25. Pourbaix, M. (1966). Atlas of electrochemical equilibria in aqueous solutions, Pergamon Press, p. 215.

26. Wranglen, G. (1984). An Introduction to Corrosion and Protection of Metals, Chapman and Hall Ltd, p. 251-252.

27. Tucker, W.C. (2006). A non chromate conversion coating process for corrosion protection of AL2024 aluminum alloys in marine environment. *RINA Conference on Advanced Marine Materials & Coatings*: p. 71-75.

28. Maddala, D. (2007). An Alternate Coating Process for Corrosion Resistance on Aluminum Alloy 2024-T3. MS Thesis, University of Rhode Island.

CHAPTER II

EXPERIMENTAL METHODS

2.1 Introduction

Aluminum (Al) and its alloys are fundamental and beneficial metals used in a wide range of industrial applications, due to their high specific strength, low density and good mechanical properties. Other than Al 2024, little to no research on electrochemical behavior has been conducted on other aluminum alloys of industrial interest, such as Al 6061 and Al 7075. Al 6061-T6 is an Al-Mg-Si alloy, which is known for its superior mechanical properties, such as high strength to weight ratio, good ductility and good corrosion resistance [1]. Al 7076 is an Al-Zn-Mg alloy, which is widely used for structural applications due to its high strength/density ratio and reasonable high fracture toughness [2].

However, the electrochemical behavior of these alloys is beginning to attract the attention of many researchers. The natural passivating oxide film on aluminum is an insufficient barrier for relatively long-term corrosion in a marine environment. Therefore, inhibitors are being used to improve protection on the surface. Traditionally, chromates have been applied in anticorrosive pre-treatments of aluminum alloys as conversion coatings [3-5]. A chromate conversion coating is a chemically grown oxide layer on the alloy substrate that provides an active barrier layer, which decreases the rate of the cathodic reaction, therefore inhibiting corrosion. However, these chromate coatings contain the hexavalent chromate ion, (Cr^{6+}) which is toxic and carcinogenic and the consequent health hazards associated with them have led to restrictions imposed on the use of these conversion coatings as well as an initiative to find

alternative methods of corrosion protection [6-11]. At present, a suitable candidate for chromate replacement has not yet been developed for Al 6061 and Al 7075, which are used for the most demanding applications.

There are several ways to inhibit corrosion including a coating that decreases the reaction rate of the substrate in which the anodic oxidation reaction is suppressed. A second method, which is of interest here, is to suppress the cathodic reduction reaction. As a result, there are no electrons available to support the anodic reaction.

A chromate-free conversion coating has successfully been developed for Al 2024-T3 using the titanate ion, which has many similarities to the chromate ion. This study mainly focuses on determining if the titanate coating process can be applied to aluminum alloys 6061-T6 and 7075-T6.

2.2 Titanate Coating Techniques

The material used throughout the research investigations was commercially produced Al 6061-T6 and Al 7075-T6, cut into 1.5-inch squares with a thickness of 0.6 inches. Typical compositions of each alloy are shown in Table 2-1 [1, 12]. The material was obtained from Q-panel. The conversion coating bath formulation and coating process, which were successfully used in the study of Al 2024 consisted of 6 g/L of potassium titanate (K_2TiO_3) and 4 g/L of sodium fluoride (NaF), which was used as an activator. The pH of the bath was adjusted to 5.5 with nitric acid and the temperature during the coating process was 60ºC. The conversion solution was prepared a day before the coating process then continuously stirred on a magnetic stirrer for 24 hours prior to coating.

The full coating process consists of a solvent cleaning and an alkaline cleaning, followed by an acid cleaning and then conversion coating. Several coating techniques were tried in order to determine the optimum coating process. A coating process similar to the Al 2024-T3 process was initially employed and includes the following series of sequential steps: (1) solvent clean with acetone, rinse in de-ionized water, (2) chemical cleaning with sodium hydroxide (NaOH) at pH of 12.5 for 10 minutes at 40ºC, rinse in de-ionized water, (3) deoxidize in proprietary solution of Smut-Go for 10 minutes at room temperature, rinse in de-ionized water, (4) conversion coating in titanate bath for 3 minutes, rinse in de-ionized water and finally (5) air dried for 24 hours. This process can be seen in Figure 2-1.

One aim of any coating process is to reduce the number of steps in the process. In this research, the alkaline cleanser was changed and the use of a proprietary acid cleaner was removed. The alkaline cleanser was enough to be sufficient pretreatment for these particular alloys for successful conversion coating.

The alternative coating technique, therefore, includes a different cleaning step. Instead of NaOH, an industrial alkaline cleanser was procured from Henkel International. Using this cleanser, a 500 mL solution and 15% by volume to water was made using 75 mL of alkaline cleanser at pH 10.6 and 425 mL of de-ionized water. The coating process includes the following: (1) solvent clean with acetone, rinse in de-ionized water, (2) chemical cleaning with alkaline cleanser at pH of 10.6 for 10 minutes at 60ºC, rinse in de-ionized water, (3) conversion coating in titanate bath for 3 minutes at pH 4.0 and 60ºC, rinse in de-ionized water and finally (4) air dried for 24 hours.

2.3 Corrosion Measurement Techniques

2.3.1 Electrochemical Impedance Testing

Once alloys had gone through the coating process, their corrosion resistance was monitored by electrochemical impedance spectroscopy (EIS). EIS measurement is a non-destructive method able to provide time dependent data on the surface properties of materials in marine environments. The test was conducted using a Gamry Instrument PC4 potentiostat connected to a computer. The test cell, which can be seen in Figure 2-2, has a glass cylinder clamped with an O-ring seal in the middle of the specimen surface to provide an exposed surface area of approximately 0.785 in^2. The cell contained about 50 mL of 0.5N sodium chloride (NaCl) electrolyte and the counter electrode was platinum foil, while the reference electrode was a saturated calomel electrode (SCE). Open circuit potential was measured for 100 seconds prior to the experiment and the impedance spectra was measured with a frequency range from 100,000 Hz to 0.01 Hz in logarithmic decrement. EIS measurements were taken over a period of 42 days (1,000 hours).

2.3.2 Potentiodynamic Tests

Potentiodynamic scans (PDS) were also conducted to determine the anodic and cathodic behavior of the alloys when titanate is in solution, but not a conversion coating. The aim is to determine if the titanate is an inhibitor to these alloys and what type of inhibitor it is. These tests were carried out in a flat sample cell, seen in Figure 2-3, using a Gamry PC4/DC105 framework potentiostat connected to a computer. The area of sample exposure was 0.4 in^2 (1 cm^2) in the flat cell and a SCE was used as the

reference electrode. Potentiodynamic experiments were carried out in oxygen purged and nitrogen purged solutions on bare Al 6061-T6 and Al 7075-T6 samples in 0.5N NaCl. Experiments were done with and without additions of titanate ions to the 0.5N NaCl electrolyte. Either oxygen or nitrogen was bubbled into the system for 1 hour prior to the experiment. Open circuit potential (OCP) was measured for 3 minutes before the actual experiment. The potential sweep started 150 mV below the open circuit for experiments without the addition of titanate and was stopped when the current density reached 10 $\mu A/cm^2$. For experiments with the addition of titanate, the potential sweep started 100 mV below the open circuit and was stopped when the current density reached 10 $\mu A/cm^2$. A scan rate of 0.1 mV/s was used throughout experimentation.

2.3.3 Crevice Corrosion

A simple test was set up in order to determine if the aluminum alloys 6061-T6 and 7075-T6 were easily susceptible to crevice corrosion in 0.5N NaCl solutions and if a titanate coating would inhibit this corrosion. Eight Al 6061-T6 and Al 7075-T6 samples (4 of each) were set up in individual 250 mL beakers. Each sample was fixed to the bottom of the beaker using a commercial modeling compound. Each beaker contained 200 mL of 0.5N NaCl. Six of the beakers contained additions of potassium titanate (K_2TiO_3) in concentrations of 1 g/L, 3 g/L or 6 g/L while the remaining two contained only 0.5N NaCl solution. Samples were left in beakers for one year. The setup can be seen in Figure 2-4.

2.4 Surface Characterization

Surface characterization was performed on immersed and conversion coated samples. To analyze the surface of conversion coated samples, a scanning electron microscope (SEM) was used with X-ray EDS capability, in which the local compositions were studied. Photographs of the immersed samples used to test for crevice corrosion were taken at various intervals over 1,000 hours. SEM imaging was done to analyze these surfaces as well. The spectra were obtained at an acceleration voltage of 20 keV.

(a) Chemical Composition of Al 6061-T6	
Element	**Wt. %**
Mg	0.8-1.2
Si	0.4-0.8
Cu	0.15-0.4
Mn	0.15 max
Fe	<0.01
Cr	0.04-0.35
Al	Bal.

(b) Chemical Composition of Al 7075-T6	
Element	**Wt. %**
Zn	5.96
Mg	2.57
Cu	1.88
Fe	0.3
Cr	0.23
Mn	0.15
Si	0.11
Ti	0.03
Al	Bal.

Table 2-1: Typical compositions of (a) Al 6061-T6 and (b) Al 7075-T6.

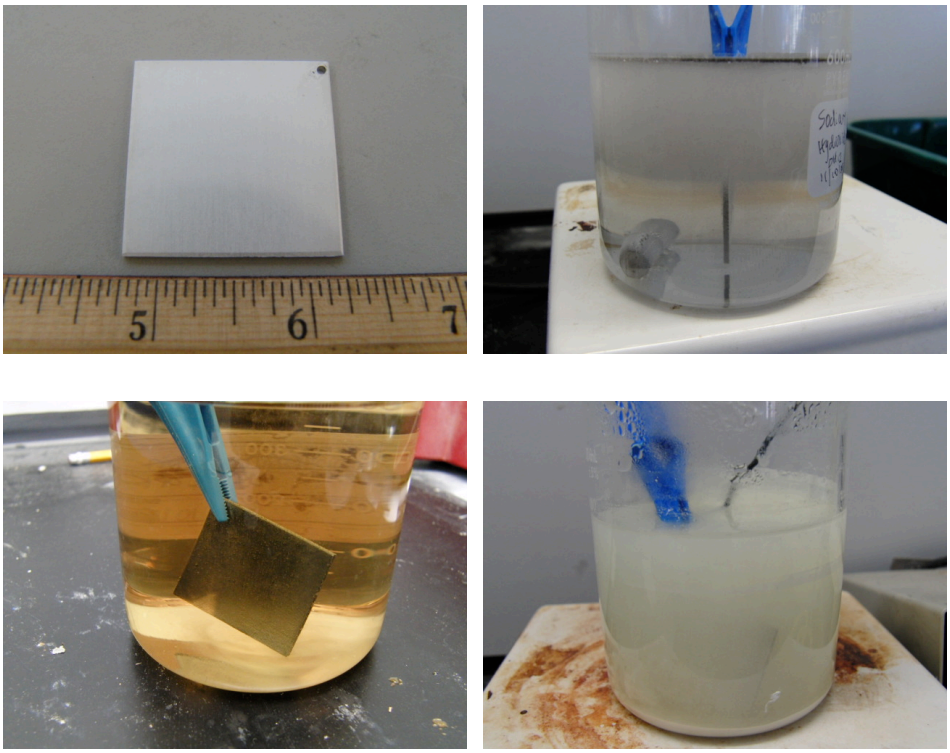

Figure 2-1: Digital images of samples (a) after acetone wash, (b) during NaOH treatment, (c) during Smut-Go treatment and (d) during conversion coating treatment.

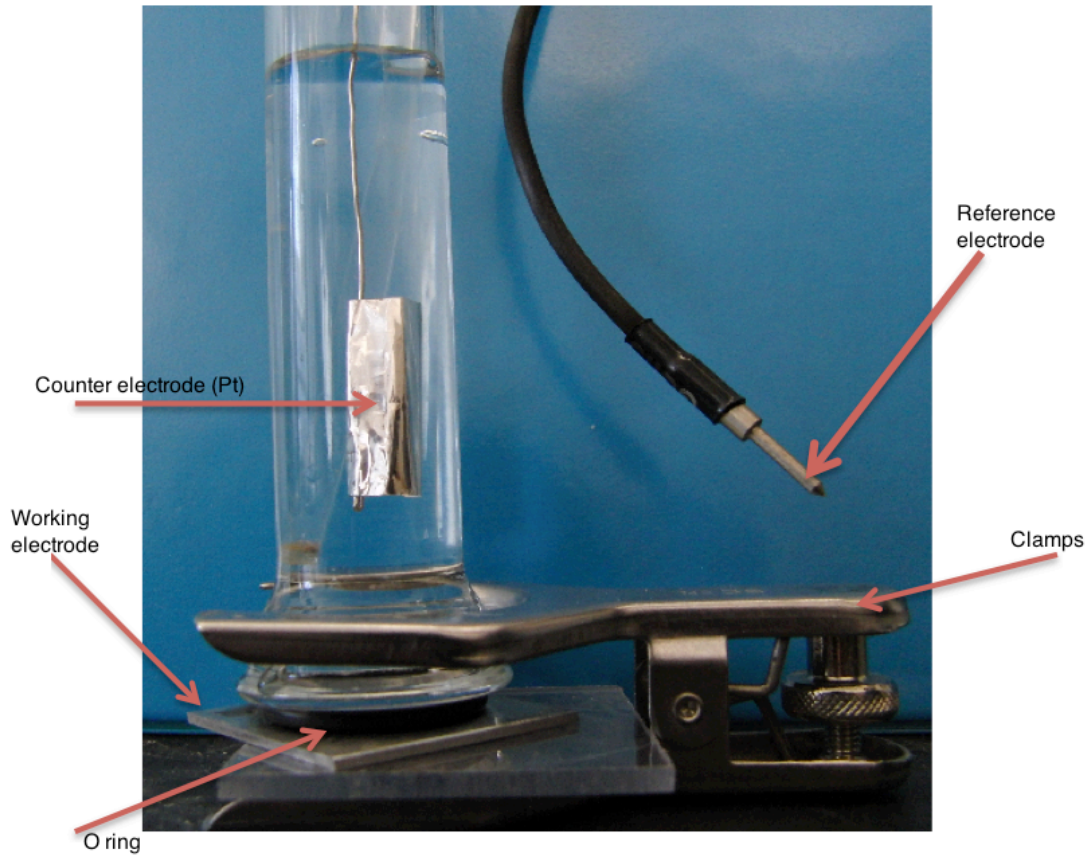

Figure 2-2: Test cell set up for electrochemical impedance spectroscopy.

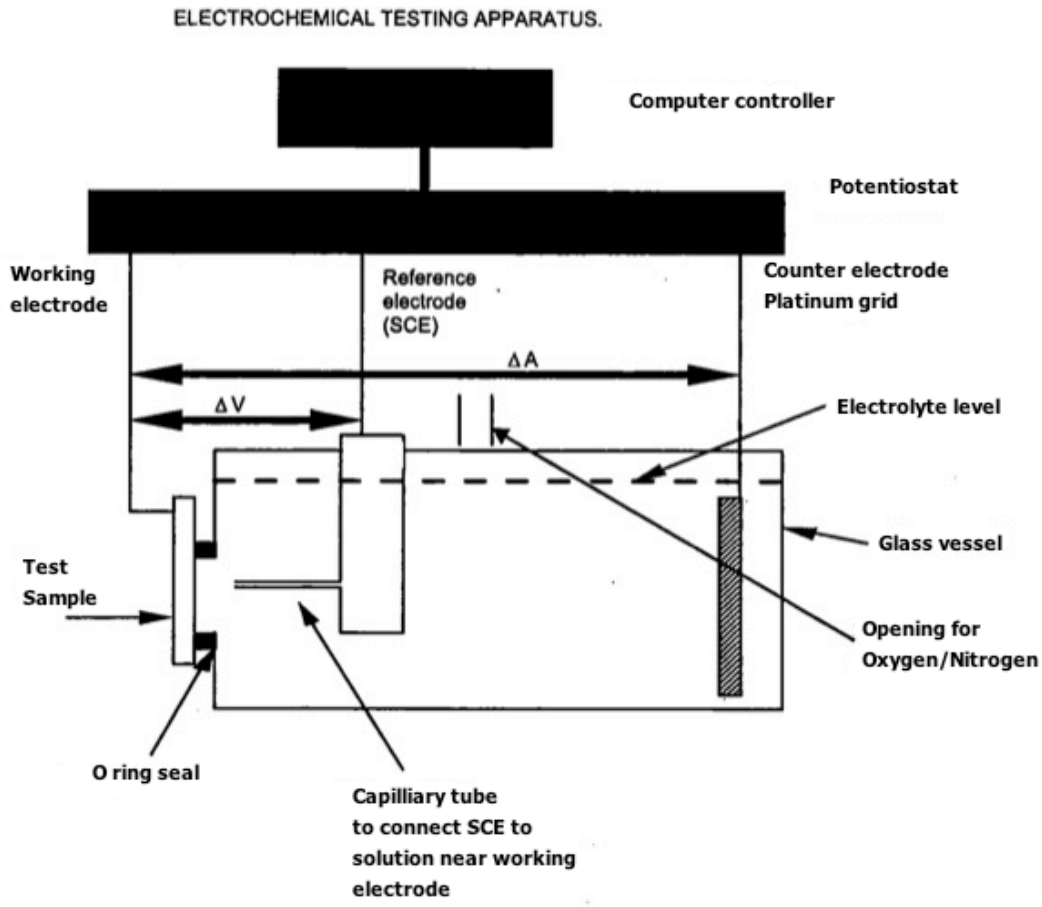

Figure 2-3: Electrochemical testing apparatus set up (flat cell) for potentiodynamic scanning.

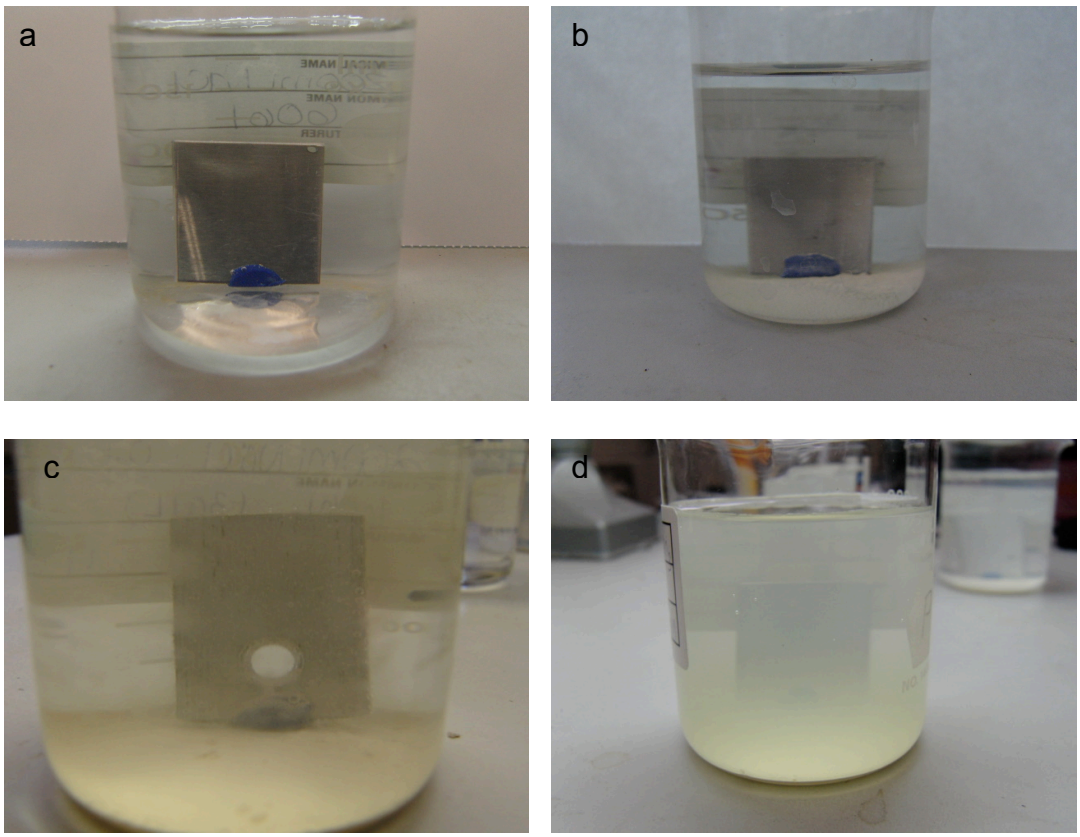

Figure 2-4: Digital images of setup for determining crevice corrosion of either Al 6061-T6 or Al 7075-T6 in (a) 200 mL of 0.5N NaCl solution, (b) 1 g/L K_2TiO_3 in 0.5N NaCl solution, (c) 3 g/L K_2TiO_3 in 0.5N NaCl and (d) 6 g/L K_2TiO_3 in 0.5N NaCl solution.

References

1. Jogi, B.F., et al. (2008). Some studies on fatigue crack growth rate of aluminum alloy 6061. *Journal of Materials Processing Technology*, 201(1-3): p. 380-384.

2. Jayaganthan, R., et al. (2010). Microstructure and texture evolution in cryorolled Al 7075 alloy. *Journal of Alloys and Compounds*, 496(1-2): p. 183-188.

3. Lytle, F.W., et al. (1995). An Investigation of the Structure and Chemistry of a Chromium-Conversion Surface-Layer on Aluminum. *Corrosion Science*, 37(3): p. 349-369.

4. Niknahad, M., S. Moradian, and S.M. Mirabedini (2010). The adhesion properties and corrosion performance of differently pretreated epoxy coatings on an aluminium alloy. *Corrosion Science*, 52(6): p. 1948-1957.

5. Xia, L., et al. (2000). Storage and release of soluble hexavalent chromium from chromate conversion coatings - Equilibrium aspects of Cr-VI concentration. *Journal of the Electrochemical Society*, 147(7): p. 2556-2562.

6. Grilli, R., et al. (2011). Corrosion behaviour of a 2219 aluminum alloy treated with a chromate conversion coating exposed to a 3.5% NaCl solution. *Corrosion Science*, 53(4): p. 1214-1223.

7. He, X.D. and X.M. Shi (2009). Self-repairing coating for corrosion protection of aluminum alloys. *Progress in Organic Coatings*, 65(1): p. 37-43.

8. Kendig, M.W. and R.G. Buchheit (2003). Corrosion inhibition of aluminum and aluminum alloys by soluble chromates, chromate coatings, and chromate-free coatings. *Corrosion*, 59(5): p. 379-400.

9. Lunder, O., et al. (2005). Formation and characterisation of a chromate conversion coating on AA6060 aluminium. *Corrosion Science*, 47(7): p. 1604-1624.

10. OSHA. "Hexavalent Chromium", Occupational Safety and Health Administration, 2009.

11. Scamans, G.M., N. Birbilis, and R.G. Buchheit (2010). Shreir's Corrosion: Corrosion of Aluminum and its Alloys, p. 2003.

12. Dey, S., M.K. Gunjan, and I. Chattoraj (2008). Effect of temper on the distribution of pits in AA7075 alloys. *Corrosion Science*, 50(10): p. 2895-2901.

CHAPTER III

EXPERIMENTAL RESULTS

3.1 Introduction

Several different methods of measuring corrosion on aluminum alloys 6061-T6 and 7075-T6 were employed in this study. Electrochemical impedance spectroscopy (EIS) was used to investigate the corrosion behavior after the conversion coating process. Approximately 35 Al 6061-T6 and 35 Al 7075-T6 samples were coated in total. Roughly 20 samples of each alloy were coated using the NaOH cleaning treatment, while the remaining were prepared using the alkaline cleanser treatment. EIS measurements were taken over a period of 42 days (1,000 hours). Potentiodynamic scans were conducted to determine the anodic and cathodic behavior of the alloys in a marine environment. These experiments were conducted in 0.5N NaCl solutions. These were purged with either oxygen or nitrogen to examine the effect of oxygen on bare Al 6061-T6 and Al 7075-T6 samples. In addition, the solutions contained either no titanate ions or had additions of titanate ions to determine their effect on electrochemical behavior.

A simple test was performed to investigate the effect of titanate ions on crevice corrosion. Samples were placed in beakers and fixed to the bottom with the commercial modeling compound then covered with 0.5N NaCl solution with varying concentrations of potassium titanate (K_2TiO_3). Samples were left in the beaker for one year. The methods of measuring corrosion employed in this study were visual observation recorded by a digital camera and surface characterization, which was

performed on immersed and conversion coated samples and conducted using a scanning electron microscope with an energy dispersed X-ray system.

3.2 Al 6061-T6

3.2.1 Electrochemical Impedance Spectroscopy

The results of the impedance measurements varied. Al 6061-T6 samples were conversion coated using two different methods. In the first method, samples were chemically cleaned with NaOH at pH 12.5 for 10 minutes at 40ºC and then submerged in a proprietary solution of Smut-Go for 10 minutes. Once cleaned, they were coated in the conversion bath at pH 5.5 for 3 minutes at 60ºC. Impedance measurements exhibited varied results. Most samples had resistances well below 10,000 ohms·cm^2 within the first week of testing. However, one sample challenged these results. On day 1, the impedance was only 45,107.8 ohms·cm^2 but over a 42-day (1,000 hours) period, the impedance increased to 138,441 ohms·cm^2. Bode plots for the sample that tested well and for a sample that tested poorly can be seen in Figure 3-1 and Figure 3-2, respectively. Samples were compared to a plain, uncoated sample.

Several scanning electron microscope (SEM) images were taken of coated and uncoated samples throughout this study in order to observe the effects of both the cleaning process and the coating. SEM images of the sample that produced high impedance magnitudes showed severe pitting on the surface. However, only minor pitting was observed on most Al 6061-T6 alloys. These can be seen in Figure 3-3.

Since the cleaning process seemed to be damaging the Al 6061-T6, a second conversion coating process involving a new cleaning step was implemented. Instead of

using NaOH and Smut-Go, samples were cleaned in an industrial alkaline cleanser at pH 10.5 for 10 minutes at 60ºC. Preliminary EIS measurements resulted in poor impedance so the pH of the titanate coating bath was decreased to 4.0. This resulted in very high impedance results. On day 1, the impedance was 270,824 ohms·cm^2. However, over the next 30 days, sodium chloride was observed to be leaking through the O-ring (Figure 2-2) and corrosion was apparent. The impedance, however, fluctuated and after 30 days, it was 265,579 ohms·cm^2. Bode plots, which compare a plain sample to the coated sample, can be seen in Figure 3-4. Surface characterization showed a smooth surface with no signs of pitting, which can be seen in Figure 3-5. Repeated results were desired but could not be achieved.

3.2.2 Potentiodynamic Scans

Potentiodynamic curves can be used to gain a better understanding of the behavior of protection of the alloy. Potentiodynamic curves for Al 6061-T6 in 0.5N NaCl solutions with and without titanate, in both oxygen-purged and nitrogen-purged systems are shown in Figure 3-6 and Figure 3-7. When purged with oxygen and in the absence of the titanate inhibitor, an open circuit potential (OCP) of approximately -700 mV SCE was measured. The cathodic limiting current density in such conditions was in the range of 5 μA/cm^2. Removing oxygen by purging the cell with nitrogen reduced the OCP to approximately -730 mV SCE. The corresponding current density decreased as well to 0.19 μA/cm^2.

When 3 g/L K_2TiO_3 was added to the system, two different reactions occurred. There was a titanium reaction and an aluminum reaction and each had their own

corresponding open circuit potentials. When purged with oxygen, the OCP of the titanium reaction was approximately -1.16 V SCE, while the OCP was -1.18 V SCE when purged with nitrogen. For the aluminum reaction, the OCP was -760 mV SCE when the system was purged with either oxygen or nitrogen. The limiting current density of the oxygen and nitrogen purged systems with titanate additions was 0.94 $\mu A/cm^2$ and 1.7 $\mu A/cm^2$, respectively.

3.2.3 Crevice Corrosion

The simple test, which was set up to determine if Al 6061-T6 is prone to crevice corrosion, yielded important results regarding protection of the alloy against crevice corrosion by the titanate ion. The sample exposed to 0.5N NaCl solution, without the addition of titanate, is slightly corroded in the region where the commercial modeling compound was present and formed a crevice. The alloy was only 0.120 inches thick in this region against a starting thickness of 0.125 inches. When varying concentrations of K_2TiO_3 were added to the NaCl solution, corrosion was not apparent anywhere, including the area where crevice corrosion was found without titanate addition. This can be seen in Figure 3-8.

3.2.4 Surface Characterization

Surface characterization and morphology of the conversion coating on Al 6061-T6 was studied using a scanning electron microscope and energy dispersive X-ray analysis. One sample cleaned with NaOH and Smut-Go had a pitted surface as well as precipitates at higher magnifications. Other samples showed no signs of pitting

but still contained precipitates. Energy dispersive (EDS) X-ray analysis showed these precipitates to be sodium fluoride (NaF) crystals. A SEM image of a precipitate along with its corresponding EDS spectrum can be seen in Figure 3-9. The sample cleaned with the industrial alkaline cleanser had no signs of pitting at high or low magnifications. However, at high magnifications, precipitates could be seen. Energy dispersive X-ray analysis showed these precipitates to be potassium fluoride (KF) crystals. The EDS spectrum can be seen in Figure 3-10 along with its corresponding SEM image.

3.3 Al 7075-T6

3.3.1 Electrochemical Impedance Spectroscopy

When cleaned with a combination of NaOH and Smut-Go and coated with a titanate bath at pH 5.5, the results were poor. On day 1, the impedance was 571.828 ohms·cm^2. Samples were only tested for 31 days due to apparent corrosion and on day 30, the impedance was 394.415 ohms·cm^2. Bode plots comparing a plain, uncoated sample and a coated sample can be seen in Figure 3-11. Similar to Al 6061-T6, SEM imaging showed pitting on the surface, although not as extreme. This can be seen in Figure 3-12.

Introducing the industrial alkaline cleanser and decreasing the pH of the coating to 4.0 also had a positive effect on Al 7075-T6 samples. On day 1, the resistance was 30,478.6 ohms·cm^2. However, similar to the Al 6061-T6 samples, sodium chloride was observed to be leaking through the O-ring and after 31 days, the final resistance was 18,532.3 ohms·cm^2, which was still exceedingly high above a

plain, uncoated sample. Bode plots comparing the two can be seen in Figure 3-13. Also similar to Al 6061-T6 was the surface characterization. As seen in Figure 3-14, the surface was smooth with no pitting. Repeated results were again unable to be obtained.

3.3.2 Potentiodynamic Scans

The potentiodynamic curves for Al 7075-T6 in 0.5N NaCl solutions with and without titanate, in both oxygen-purged and nitrogen-purged systems can be seen in Figure 3-15 and Figure 3-16. When the system was purged with oxygen and no titanate was added to the cell, the OCP measured was approximately -700 mV SCE. The corresponding cathodic limiting current density was about 20 $\mu A/cm^2$. Removing oxygen by purging the cell with nitrogen resulted in a lower OCP of -820 mV SCE and a lower current density of 1.0 $\mu A/cm^2$.

When 3 g/L K_2TiO_3 was added to the cell, both a titanium and an aluminum reaction occurred, each with their own corresponding open circuit potential. When purged with oxygen, the OCP of the titanium reaction was approximately -1.15 V SCE, which also happened in the case of the system purged with nitrogen. For the aluminum reaction, the OCP was -760 mV SCE for the oxygen-purged system. Removing oxygen by purging the system with nitrogen increased the OCP slightly to -740 mV SCE. The limiting current density of the oxygen and nitrogen purged systems with titanate additions was 2.25 $\mu A/cm^2$ and 1.9 $\mu A/cm^2$, respectively.

3.3.3 Crevice Corrosion

The simple test also provided useful information regarding the titanate ion decreasing crevice corrosion for Al 7075-T6. The sample exposed to 0.5N NaCl solution, without the addition of titanate, was severely corroded where the commercial modeling compound created a crevice. The measured thickness of the crevice was 0.049 inches against a starting thickness of 0.0625 inches. Adding varying concentrations of titanate to the NaCl solution did not seem to corrode the samples anywhere, including the region where crevice corrosion was found without the addition of titanate. Digital images of each sample can be seen in Figure 3-17.

3.3.4 Surface Characterization

Surface characterization and morphology of the conversion coating on Al 7075-T6 were studied using energy dispersive X-ray analysis and scanning electron microscope imaging. Similar to the Al 6061-T6 alloy, SEM imaging showed precipitates on the surface whether the alloy was cleaned with NaOH and Smut-Go or the alkaline cleanser. Energy dispersive X-ray analysis indicated that the precipitates on the surfaces cleaned with NaOH and Smut-Go were NaF crystals. A SEM image of a precipitate along with its corresponding EDS spectrum can be seen in Figure 3-18. On surfaces cleaned with the industrial alkaline cleanser, KF crystals were seen, which are shown in Figure 3-19.

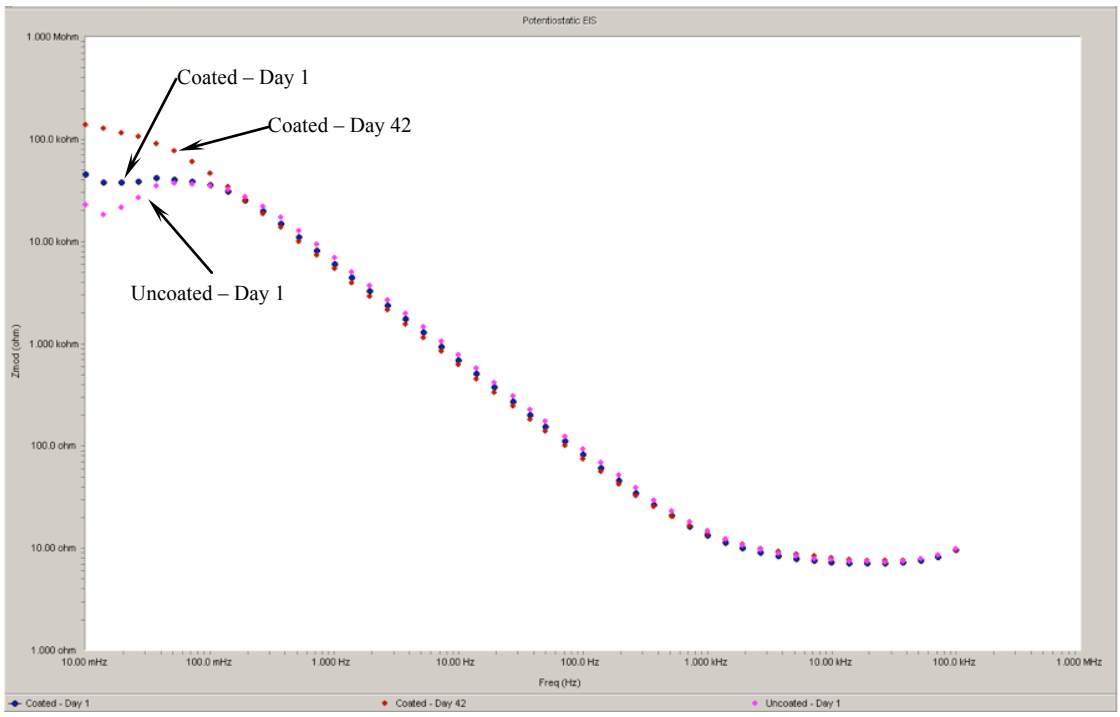

Figure 3-1: Al 6061-T6 Bode plot comparing coated sample, which exhibited high impedance magnitudes, to an uncoated sample. Coated sample was cleaned with NaOH and Smut-Go and coated in titanate bath with pH 5.5.

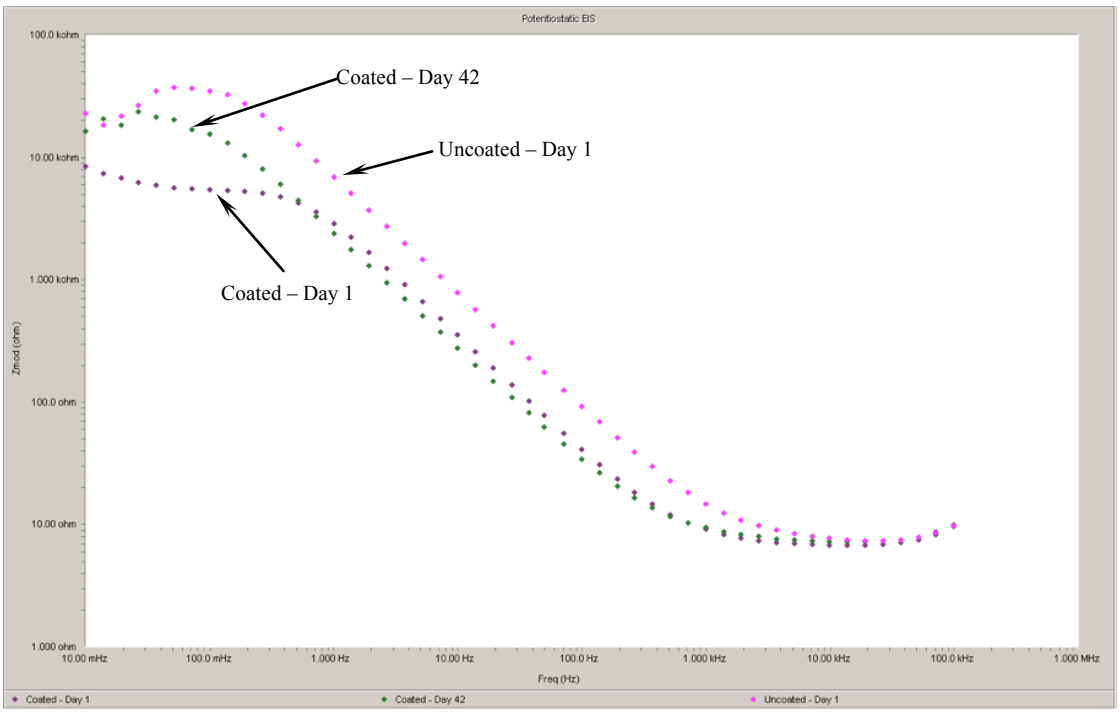

Figure 3-2: Al 6061-T6 Bode plot comparing coated sample, which exhibited very low impedance magnitudes, to an uncoated sample. Coated sample was cleaned with NaOH and Smut-Go and coated in titanate bath with pH 5.5.

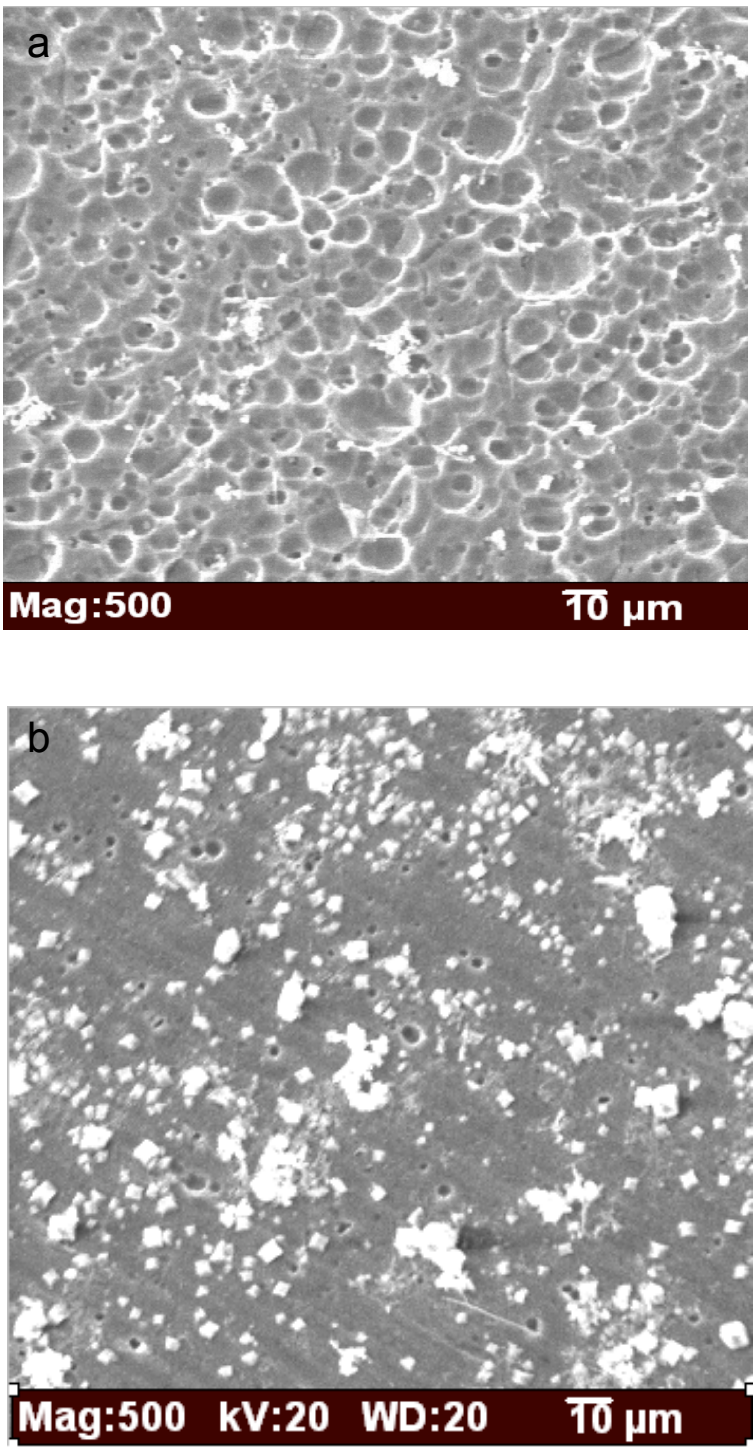

Figure 3-3: SEM images of Al 6061-T6 samples cleaned in NaOH and coated in titanate bath with pH 5.5, which produced (a) good resistances and (b) poor resistances. Samples were exposed to 0.5N NaCl solution for 42 days (1,000 hours).

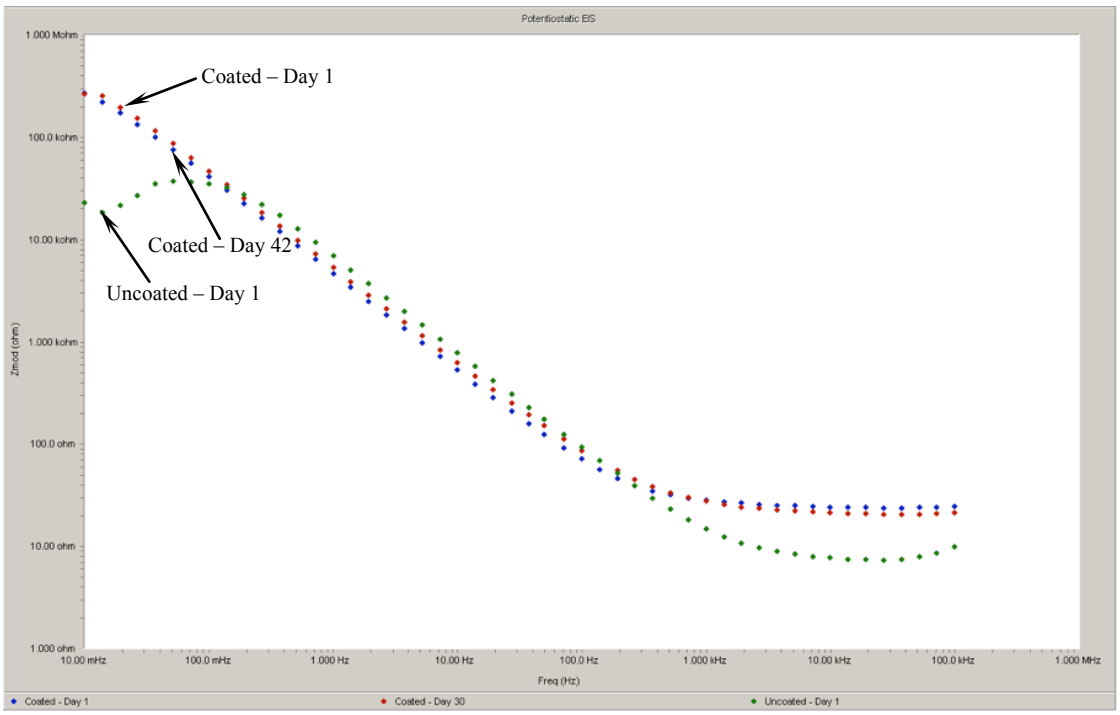

Figure 3-4: Al 6061-T6 Bode plot comparing a coated sample to an uncoated sample. Coated sample was cleaned in alkaline cleanser coated in titanate bath with pH 4.0.

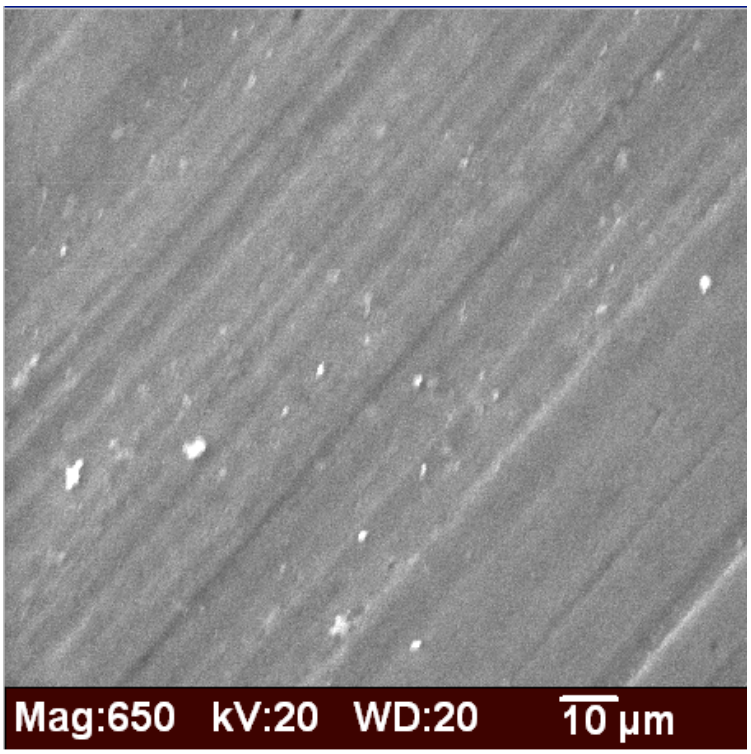

Figure 3-5: SEM image of Al 6061-T6 sample after 31 days of exposure to 0.5N NaCl. Sample was cleaned in alkaline cleanser and coated in titanate bath with pH 4.0.

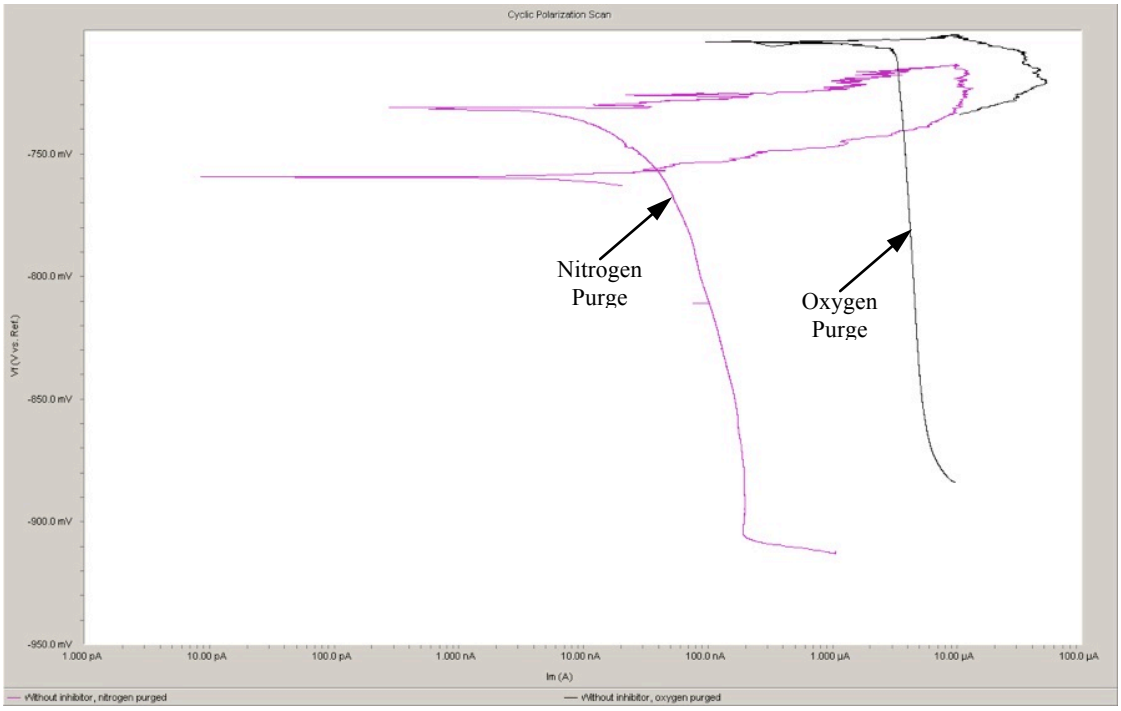

Figure 3-6: Al 6061-T6 potentiodynamic curves in 0.5N NaCl solution without titanate in both nitrogen and oxygen purged solutions.

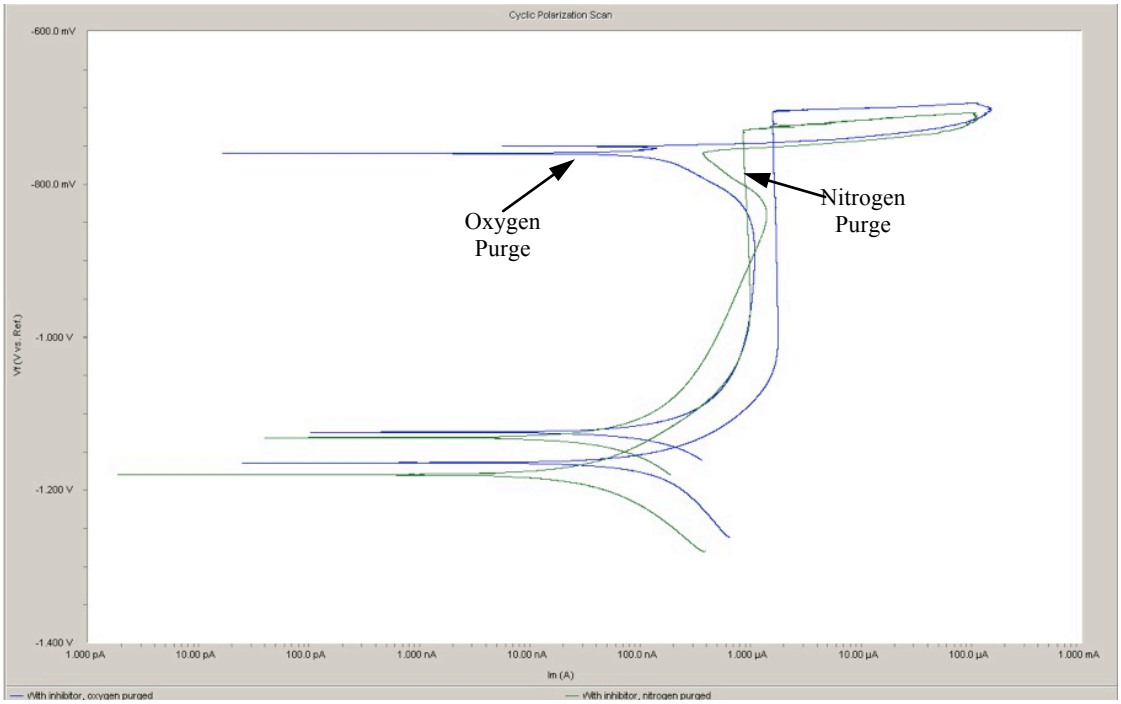

Figure 3-7: Al 6061-T6 potentiodynamic curves in 0.5N NaCl solutions with titanate in both nitrogen and oxygen purged solutions.

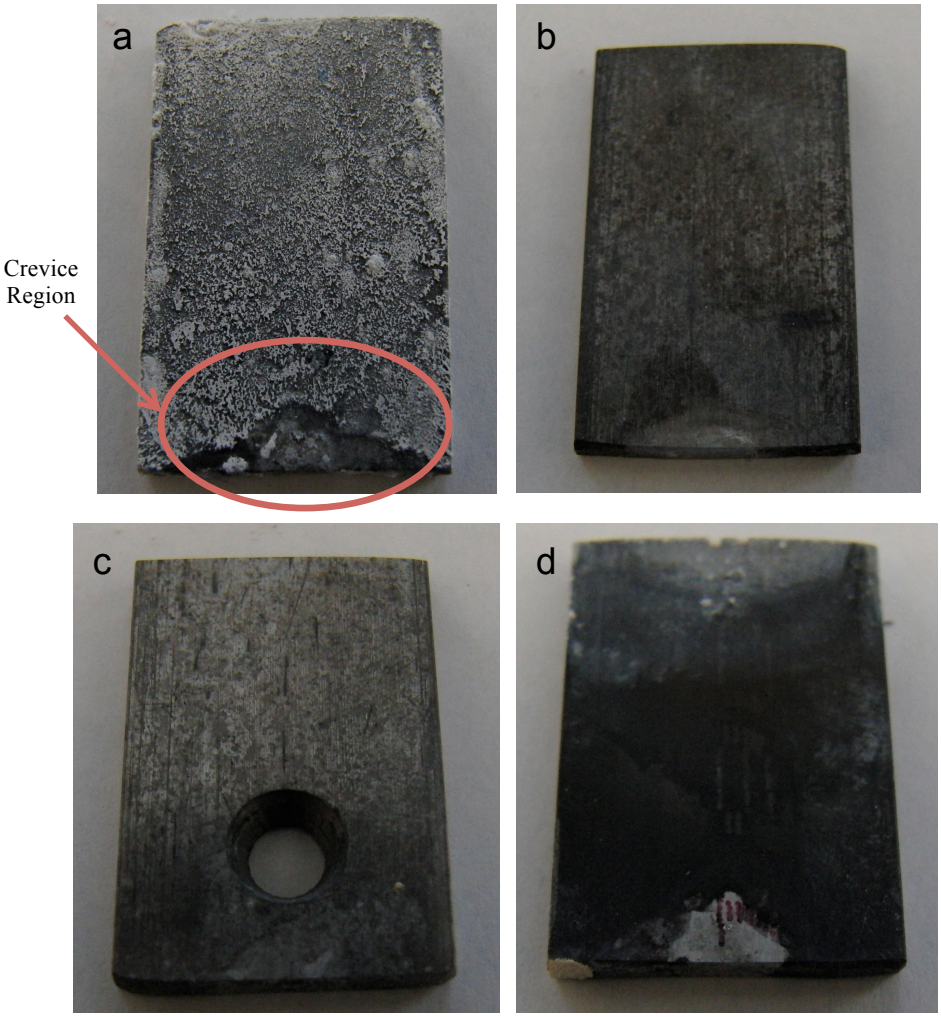

Figure 3-8: Digital images of Al 6061-T6 samples after one year in solutions of (a) 0.5N NaCl, (b) NaCl + 1 g/L K_2TiO_3, (c) NaCl + 3 g/L K_2TiO_3 and (d) NaCl + 6 g/L K_2TiO_3. Crevice region of (a) measured 0.120" against 0.125" for titanate samples.

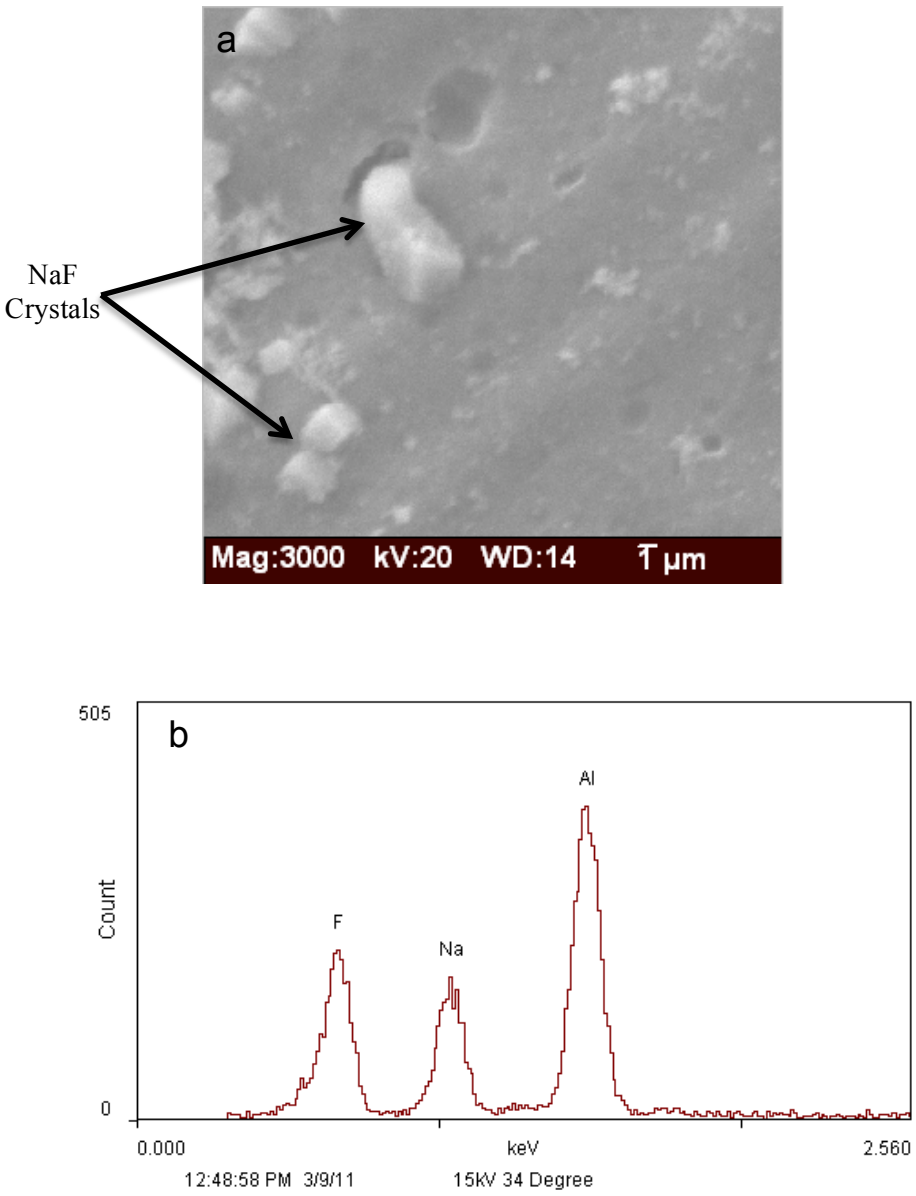

Figure 3-9: (a) SEM image of NaF crystals on Al 6061-T6 alloy cleaned in NaOH and coated in titanate bath with pH 5.5 and (b) EDS spectra of NaF crystals.

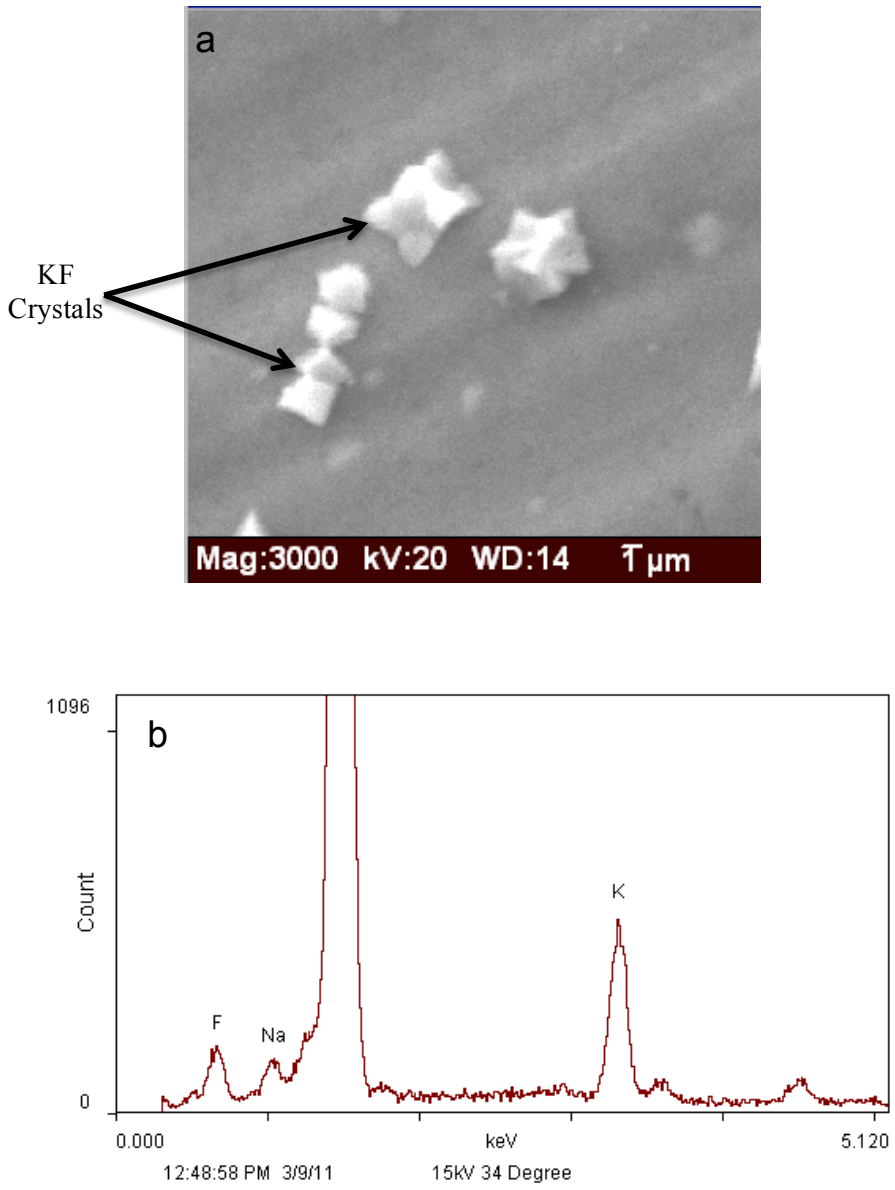

Figure 3-10: (a) SEM image of KF crystals on Al 6061 alloy cleaned in alkaline cleanser and coated in titanate bath with pH 4.0 and (b) EDS spectra of KF crystals.

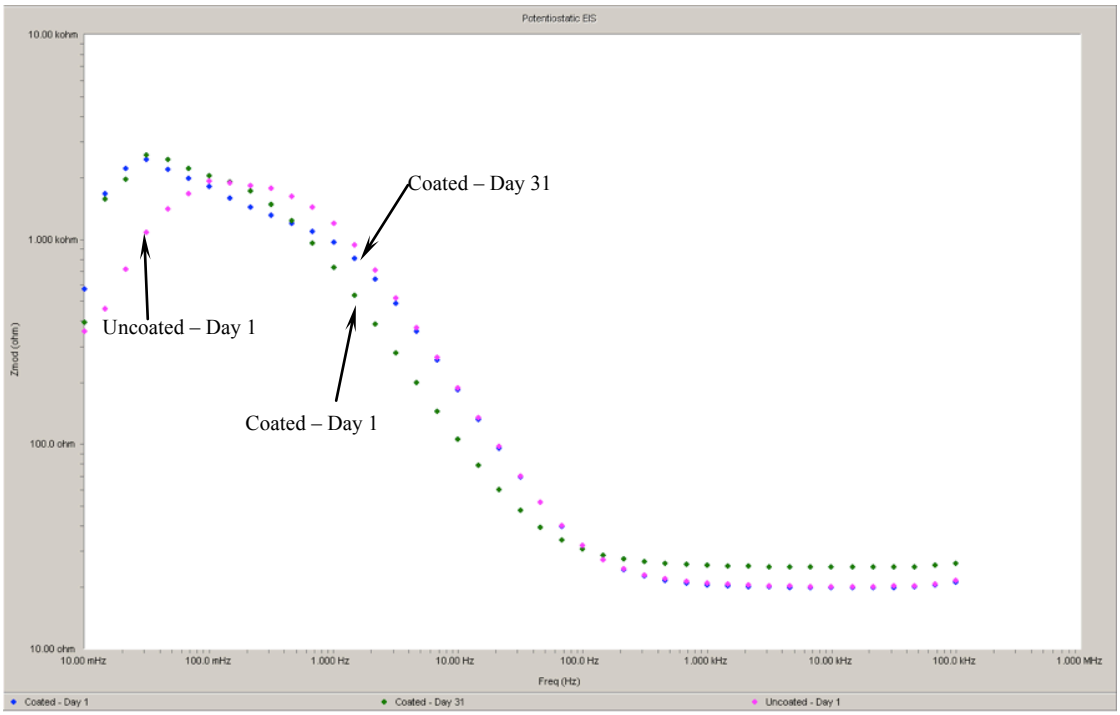

Figure 3-11: Al 7075-T6 Bode plot comparing a coated sample to an uncoated sample. Coated sample was cleaned with NaOH and Smut-Go and coated in titanate bath with pH 5.5.

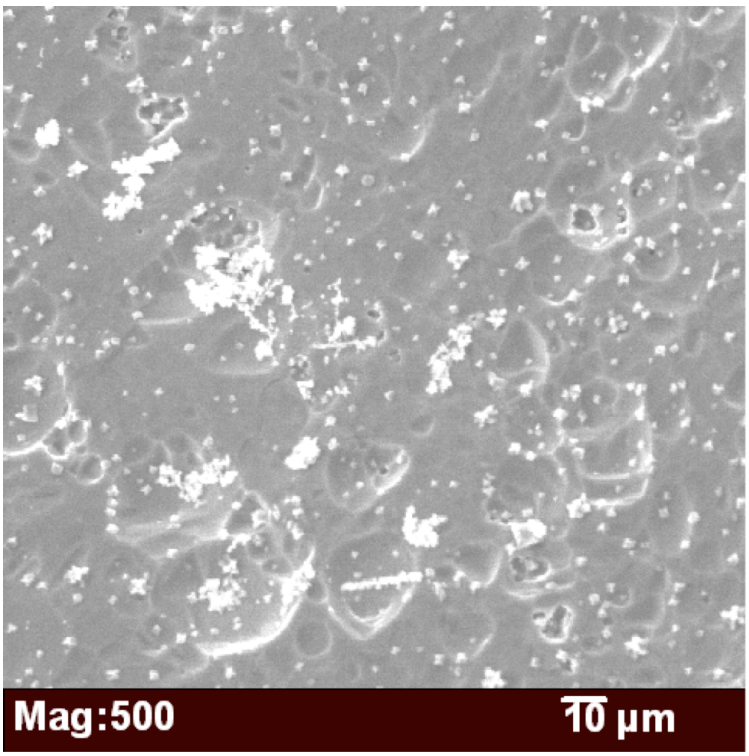

Figure 3-12: SEM image of pitting on Al 7075-T6 sample cleaned in NaOH and coated in titanate bath with pH 5.5. Sample was exposed to 0.5N NaCl solution for 42 days (1,000 hours).

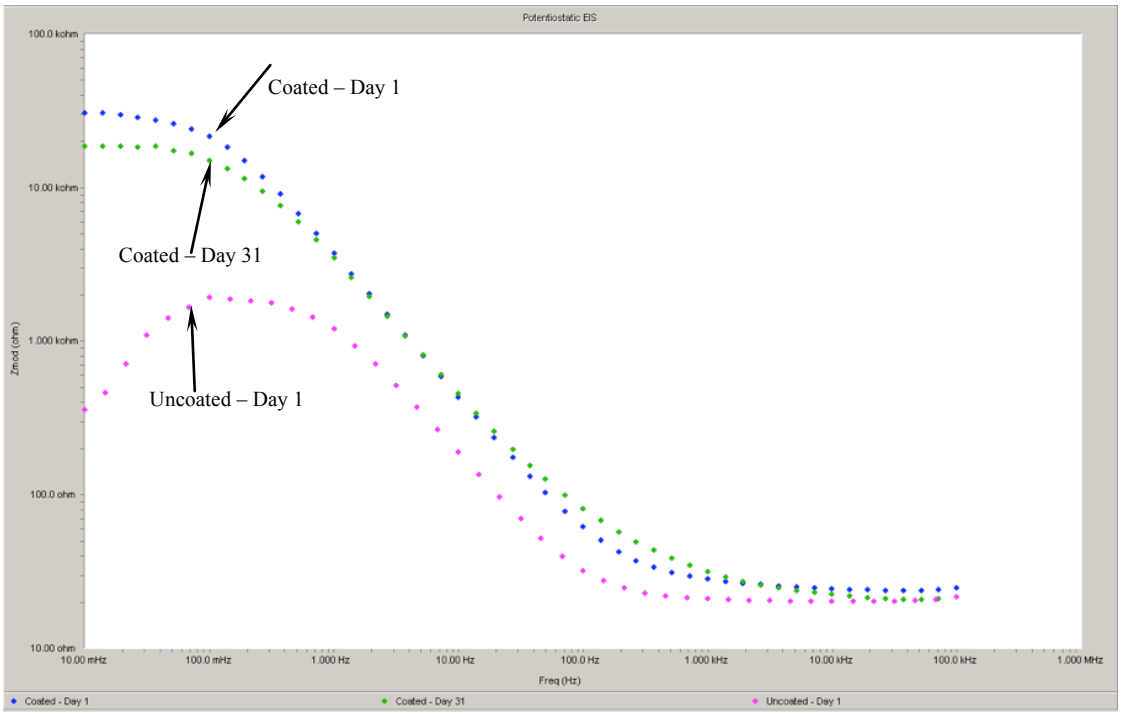

Figure 3-13: Al 7075-T6 Bode plot comparing a coated sample to an uncoated sample. Coated sample was cleaned in alkaline cleanser coated in titanate bath with pH 4.0.

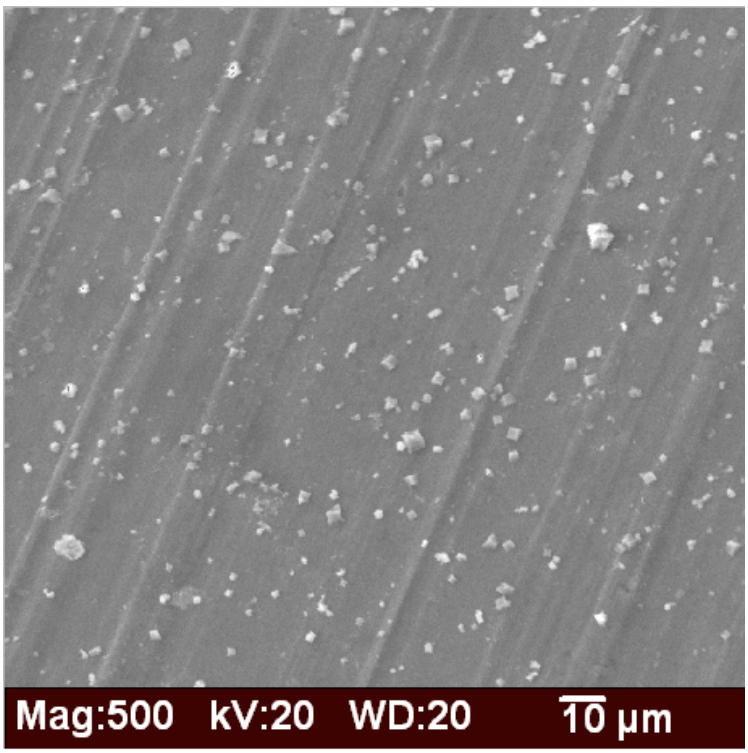

Figure 3-14: SEM image of Al 7075-T6 after 31 days of exposure to 0.5N NaCl solution. Sample was cleaned in alkaline cleanser and coated in titanate bath with pH 4.0.

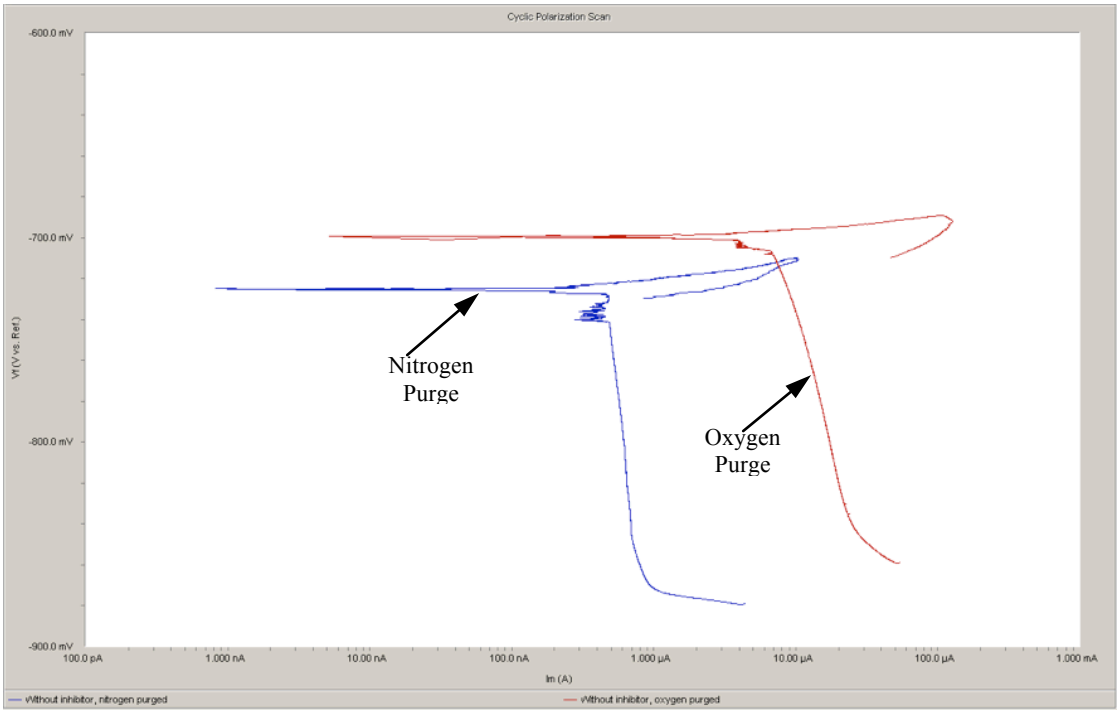

Figure 3-15: Al 7075-T6 potentiodynamic curves in 0.5N NaCl solution without titanate in both nitrogen and oxygen purged solutions.

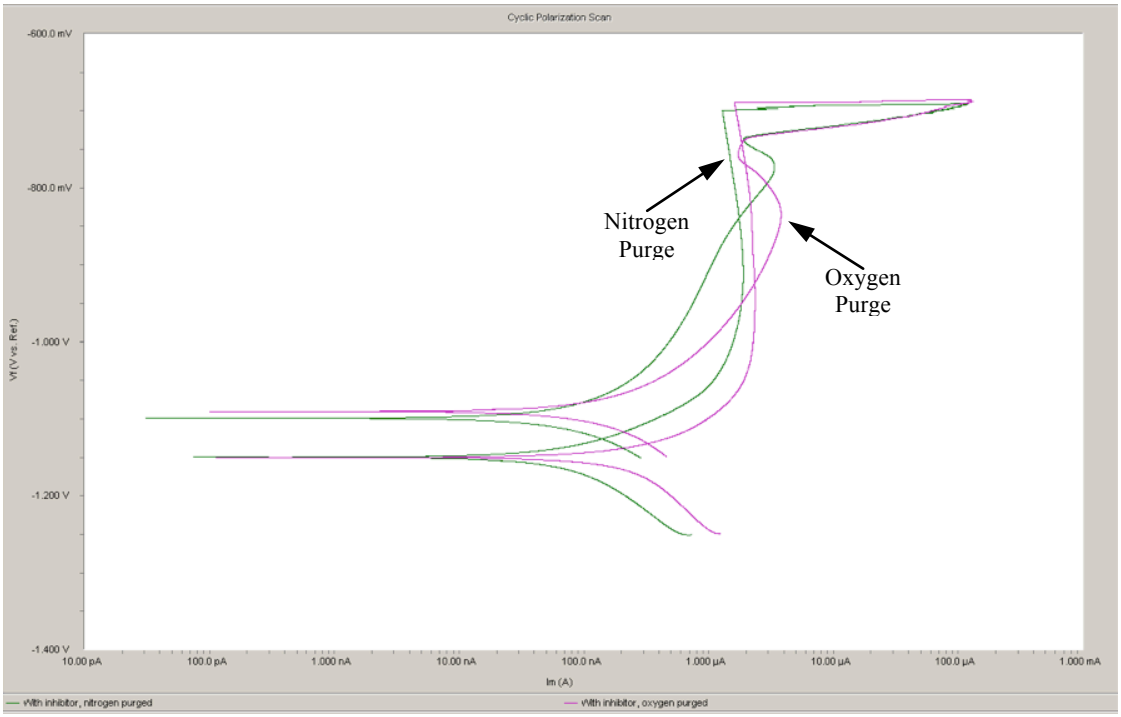

Figure 3-16: Al 7075-T6 potentiodynamic curves in 0.5N NaCl solution with the addition of titanate in both nitrogen and oxygen purged solutions.

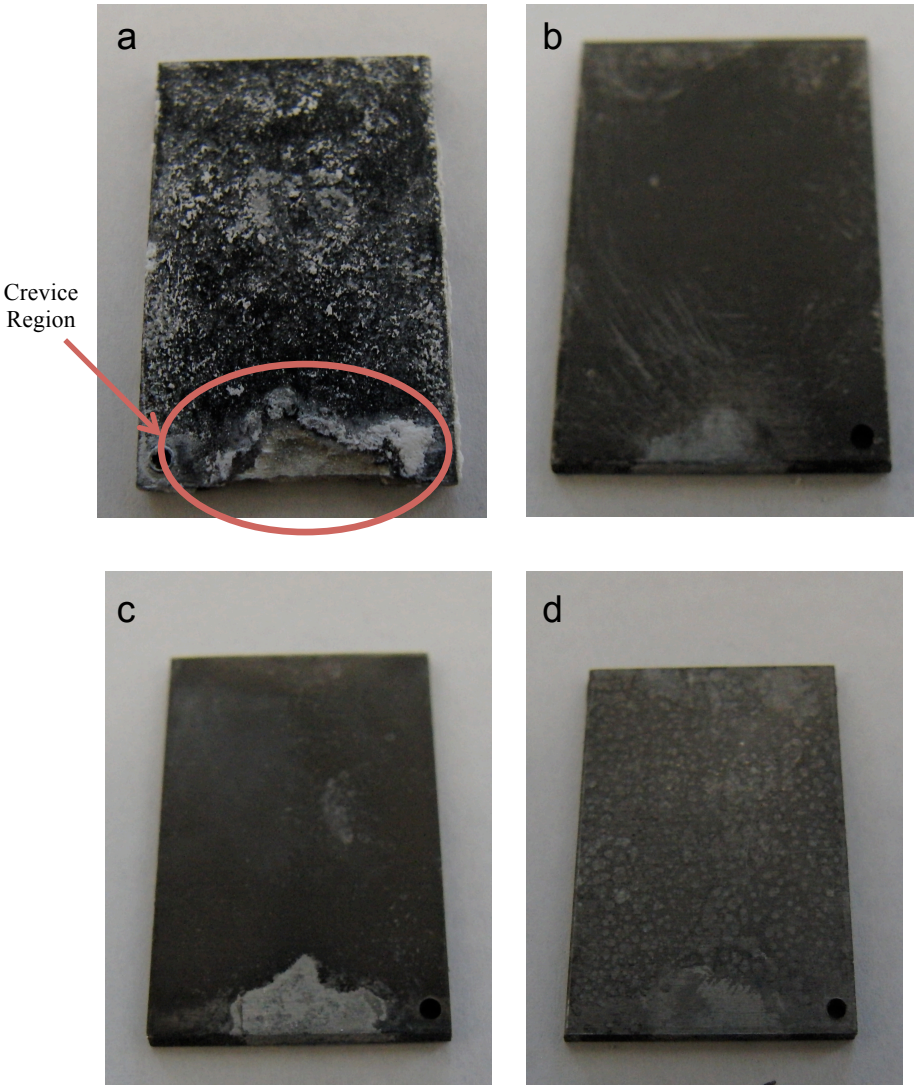

Figure 3-17: Digital images of Al 7075-T6 samples after one year in solutions of (a) 0.5N NaCl, (b) NaCl + 1 g/L K_2TiO_3, (c) NaCl + 3 g/L K_2TiO_3 and (d) NaCl + 6 g/L K_2TiO_3. Crevice region in (a) with NaCl only measured 0.049" compared to 0.0625" for titanate samples.

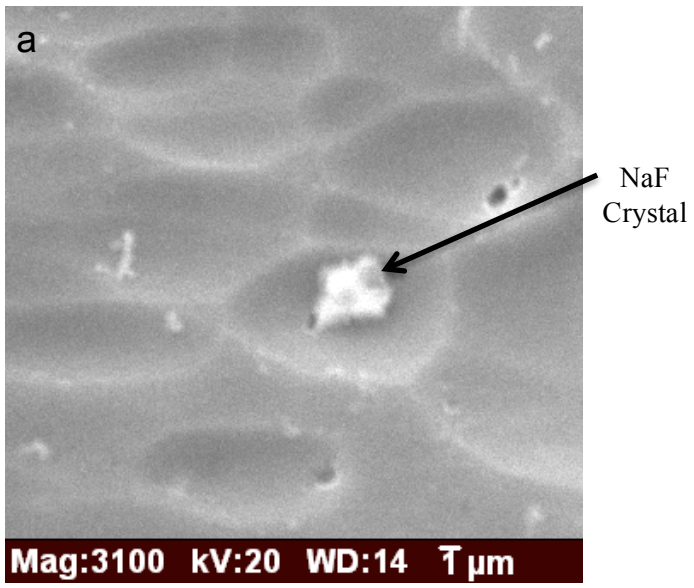

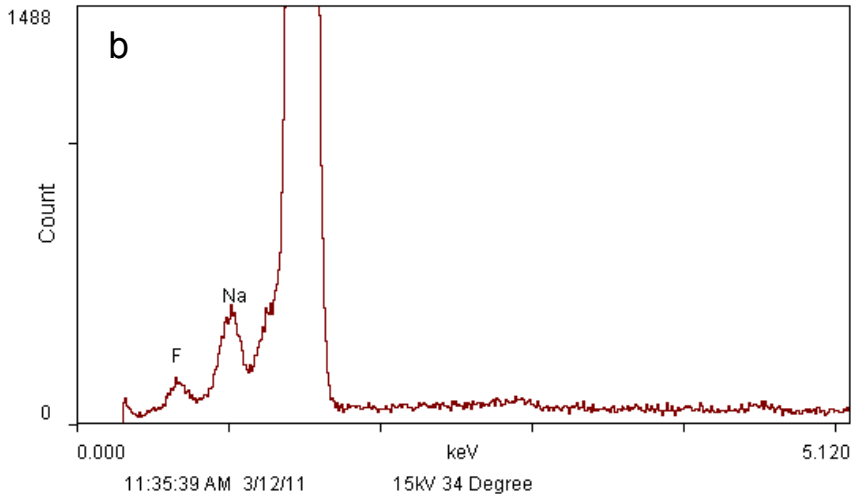

Figure 3-18: (a) SEM image of NaF crystal on Al 7075 alloy cleaned in NaOH and coated in titanate bath with pH 5.5 and (b) EDS spectra of NaF crystal.

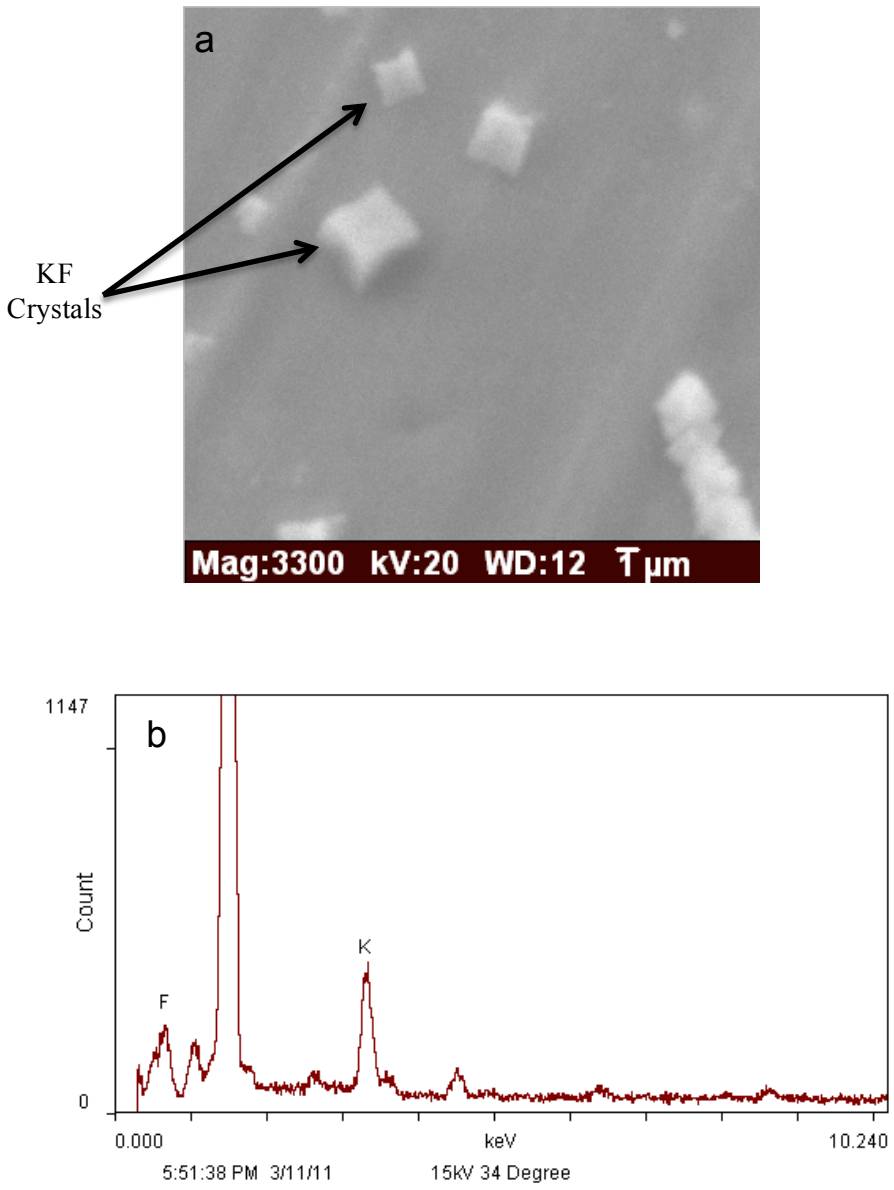

Figure 3-19: (a) SEM image of KF crystals on Al 7075 alloy cleaned in alkaline cleanser and coated in titanate bath with pH 4.0 and (b) EDS spectra of KF crystals.

CHAPTER IV

DISCUSSION

4.1 Crevice Corrosion

General conditions for crevice corrosion include a stagnant halide ion containing solution and a narrow gap between two surfaces, one of which is metal [1]. In this study, a test was conducted in order to determine if both Al 6061-T6 and Al 7075-T6 are prone to crevice corrosion when exposed to NaCl solution as well as the effect of the titanate ion on crevice corrosion. A sample was placed in a stagnant solution (NaCl) and fixed to the bottom of a beaker using a commercial modeling compound. Therefore, the surfaces, the metal alloy and the modeling compound, formed a crevice. Inside the crevice region, dissolved oxygen could not easily be replaced. The region inside the crevice could not support a cathodic reaction but could still support an anodic reaction, while outside the crevice region, the cathodic reaction proceeded but the anodic reaction ceased. Consequently, an electrical charge imbalance took place between the high positive charge from the metal ions within the crevice and the negative charge outside the crevice, allowing chloride ions into the crevice. Therefore, the corrosion rate inside the crevice increased.

The final thickness of the Al 6061-T6 sample was 0.120 inches against a starting thickness of 0.125 inches. The initial thickness of the Al 7075-T6 sample was 0.0625 inches. After being exposed to NaCl solution, the crevice region was reduced to 0.049 inches. Crevice corrosion on both Al 6061-T6 and Al 7075-T6 can be seen in Figure 3-7a and Figure 3-14a, respectively.

When varying concentrations of potassium titanate (K_2TiO_3) were added to 0.5N NaCl solution, crevice corrosion was not apparent. This suggests that even at small concentrations, the titanate ion inhibits crevice corrosion. Digital images can be seen in Figure 3-7(b-d) and Figure 3-14(b-d) for Al 6061-T6 and Al 7075-T6, respectively.

This test also suggests that the titanate ion would be a good candidate for a conversion coating solution if it can be applied effectively. In a test such as this one, the crevice corrosion can start anywhere where the crevice and the solution conditions become acidic. Clearly the titanate ion is a good inhibitor of crevice corrosion.

4.2 Potentiodynamic Scans

To investigate the effect of the titanate ion in electrochemical behavior, potentiodynamic curves for Al 6061-T6 in 0.5N NaCl solution with and without titanate in both oxygen and nitrogen purged conditions were conducted. Data from this study are shown in Figure 3-5 and Figure 3-6. Results for Al 7075-T6 investigated in the same conditions are shown in Figure 3-12 and Figure 3-13. The data for both alloys is summarized in Table 4-1. The analysis of these curves is difficult once the titanate ion is added to the system. For these alloys, the addition of the titanate added a second reaction at low potentials in addition to the redox reaction associated with the aluminum in the absence of the titanate. The reactions suspected to be occurring are a mixture of cathodic reductions and anodic oxidation reactions for the species present. When the potential is more negative than -1.15 V, the cathodic reaction takes place as titanate ions are reduced to form titanium on the surface of the aluminum alloy.

$$Ti^{4+} + 4e^- \rightarrow Ti \quad (1)$$

When the potential is more positive than -1.15 V, the titanium anodic reaction is initiated and titanium is oxidized to create titanium ions, which react with oxygen to form an oxide passivating layer.

$$Ti + O_2 \rightarrow TiO_2 \quad (2)$$

It can be hypothesized that the titanate ion displaces other species, forming a film on the alloy surface, which then passivates the surface and impedes additional electron transfer by making ion movement difficult. The effect of this film is shown by the large reduction in the cathodic current density. For the Al 6061-T6 alloy, the cathodic current density decreased from 5 $\mu A/cm^2$ to 0.94 $\mu A/cm^2$. For the Al 7075-T6 alloy, the current density decreased from 20 $\mu A/cm^2$ to 2.25 $\mu A/cm^2$ when titanate was added to the system and the system was purged with O_2.

When the potential is more positive than -700 mV, the aluminum anodic oxidation reaction is taking place.

$$Al \rightarrow Al^{3+} + 3e^- \quad (3)$$

The TiO_2 film cannot resist this reaction and is broken down, exposing aluminum.

Removing oxygen by purging the system with nitrogen results in a larger cathodic current density, which may be related to the electrochemical reduction of titanate ions. Comparing both oxygen and nitrogen purged cathodic polarization curves, it can be hypothesized that the presence of oxygen in the solution produces the oxide based film faster than lower oxygen levels can, which results in lower cathodic currents with higher oxygen levels in solution.

The potentiodynamic data indicate one possible mechanism for the titanate conversion coating. The low primary passivation potential of -1.18 V SCE combined with very low critical current densities indicate that the titanate ion is a cathodic inhibitor. Cathodic inhibitions reduce one of the necessary components for corrosion, namely the cathodic reaction rate. As this is lowered, the anodic reaction cannot be supported. Chromates are suspected to work in a similar manner [2] by acting as a cathodic inhibitor. Another requirement is 'self-healing', the ability to repair defects [3]. This mechanism can be seen in Figure 4-1.

4.3 Electrochemical Impedance Spectroscopy

When choosing aluminum alloys for industrial use, the 6xxx series is highly suitable in various applications due to its good resistance to corrosion [4]. Electrochemical impedance data indicates that a plain, uncoated Al 6061-T6 sample has a relatively high impedance magnitude of 22,625.4 ohms·cm^2 on day 1. Therefore, samples that have undergone a conversion coating process to enhance corrosion resistance should have impedance measurements well above that of a plain, uncoated sample.

Electrochemical impedance data displayed as Bode phase plots in 0.5N NaCl solution for Al 6061-T6 alloys, which were chemically cleaned with NaOH at pH 12.5 and titanate conversion coated at 5.5 pH for 3 minutes is presented in Figure 3-1. These plots show time dependent data for two samples, one exhibiting high impedances and a second sample, which showed very poor impedances as a function of time. When examined in a scanning electron microscope, severe pitting was

observed on the sample that produced high impedance magnitudes (Figure 3-2a). Only minor pitting was seen, however, on most samples throughout the study. However, their impedance and corrosion resistance was low. The presence of pitting alone was not sufficient to produce a conversion coating that did not increase corrosion resistance. One possible explanation is that the severity of the local surface changes may harm the corrosion resistance. Consequently, few pits with severe surface profile changes may disrupt the coating and impede resistance by initiating flaws. This indicates a non-pitting cleaning stage has to be required.

Unlike the 6xxx series, alloys in the 7xxx series are more susceptible to corrosion especially those containing copper, such as Al 7075. This decrease in corrosion resistance is indicated by an electrochemical impedance for a plain, uncoated sample of a 354.876 ohms·cm^2 on day 1, in comparison to Al 6061-T6, which was 22,625 ohms·cm^2 on day 1. Electrochemical impedance data for Al 7075-T6 cleaned in NaOH and titanate coated with pH 5.5 is presented in Figure 3-10. EIS measurements after the titanate coating bath indicated very low impedance magnitudes.

Electrochemical impedance data displayed as Bode phase plots in 0.5N NaCl solution for Al 6061-T6 and Al 7075-T6 alloys, which were cleaned in an alkaline cleanser with pH 10.5 and titanate conversion coated at 4.0 pH for 3 minutes is presented in Figure 3-3 and Figure 3-12, respectively. Reducing the steps of the coating process to using just an alkaline cleanser instead of both NaOH and Smut-Go produced high impedance magnitudes on only one sample of Al 6061-T6 throughout the study. Relatively high resistances were seen on an Al 7075-T6 sample but were still low enough to be considered poor data.

4.4 Possible Reasons for Poor Coating Performance

4.4.1 Mechanical

There are several possible reasons for poor resistance measurements, which can be attributed to the titanium coating on the surface of the aluminum alloy. Possible mechanical explanations include pitting on the surface. In this study, sodium hydroxide (NaOH) attacks the surface and this attack results in pits. Earlier studies did not indicate this severity of attack but this was on Al 2024-T3, a copper rich alloy [5]. As stated in the previous section, if the severity of the local surface changes, the corrosion resistance may be harmed.

SEM imaging shows different types of pitting on the surface, single pits as well as concentrations of multiple pits. Single pits have a hemispherical shape where the majority is underneath the surface. There is an extreme angle change and a bad surface profile, which tends to be sharper. Where there are multiple pits, more material is removed, which leads to the removal of the surface, allowing for a smoother coating over the pitted surface. SEM imaging and EIS measurements indicated that the sample with multiple pits had good corrosion resistance, while samples with single pits throughout lead to low impedance magnitudes. When a second cleaning system is employed to remove the NaOH, no pitting was found yet the EIS indicated that the conversion coating was still not reliable. This suggests another mechanism may be involved with poor coating performance. These mechanisms can be seen in Figure 4-2.

4.4.2 Microstructure

One other possible reason for coating failure is the presence of second phase particles on the surface. If there are Mg_2Si (Al 6061) or $MgZn_2$ (Al 7075) particles on the surface, there will be a break in the coating and corrosion will occur. As the titanate ion inhibited crevice corrosion on these alloys, it appears that it can protect against these microstructural features, which will always be present on the surface. This mechanism can be seen in Figure 4-3.

4.4.3 Chemical Precipitates

Low resistance measurements on Al 6061-T6 and Al 7075-T6 alloys in this study can be explained by the surface characterization of each alloy. SEM imaging showed large clusters of precipitates on the surfaces. A simple mechanism depicting a damaging precipitate on the surface can be seen in Figure 4-4. Energy dispersive X-ray analysis indicated that these precipitates were fluoride (F^-) crystals. Fluoride ions are known to be extremely aggressive towards titanium [6, 7]. High concentrations of fluoride ions will destroy the oxide film that was chemically grown by the titanium bath. If there are damaging precipitates on the surface of the alloy, such as fluoride, coating failure will always occur, which will always lead to corrosion, which can be confirmed by EIS measurements in this study.

For Al 6061-T6 and Al 7075-T6 samples cleaned with NaOH and Smut-Go and then titanate coated with pH 5.5, energy dispersive X-ray analysis indicated that the precipitates on the surface were sodium fluoride (NaF), which was used as an activator in the conversion coating bath.

On samples cleaned with the alkaline cleanser and then titanate coated with pH 4.0, energy dispersive X-ray analysis indicated that the precipitates were potassium fluoride (KF), which seemed to have formed during the coating step when the fluoride ion attached itself to the potassium from the potassium titanate (K_2TiO_3). On the Al 6061-T6 sample that produced high impedance magnitudes, SEM imaging showed a small concentration of KF precipitates. On all other samples with poor coating performance, higher concentrations were seen. It seems that as a result of high concentrations of NaF or KF precipitates, impedance magnitudes were very low.

4.5 Conclusions

A test, which was conducted to determine if Al 6061-T6 and Al 7075-T6 are prone to crevice corrosion, yielded critical results regarding the protection of Al 6061-T6 and Al 7075-T6 against crevice corrosion by the titanate ion. It has been determined that the titanate ion protects these alloys against crevice corrosion in a marine environment.

Titanate based conversion coatings hold promise as a replacement for chromates on Al 6061-T6 and Al 7075-T6 alloys as they show passive film that inhibits the surface from corrosion. The potentiodynamic study revealed that the film protects the alloy surface. However, electrochemical impedance spectroscopy exhibited varied results and impedance magnitudes were typically low. It seems that pitting on the surface did not have an effect on corrosion resistance, which is confirmed by the varied EIS measurements.

It can be concluded, however, that low impedance magnitudes can be attributed to the precipitation of fluoride ions during the coating process, which significantly inhibit corrosion protection. Any surface with sodium fluoride precipitates present will corrode. Further investigation will be required in order to determine an optimum conversion bath, which will produce impedance magnitudes comparable to those measured for the Al 2024-T3 alloy.

In conclusion, once an optimum coating process for these alloys is determined, further work will be needed to turn the process into an industrially accepted system, in which an optimized and consistent coating process will meet all the necessary requirements.

	Open Circuit Potential (OCP)		Current Density (*i*)	
	Nitrogen (N_2)	Oxygen (O_2)	Nitrogen (N_2)	Oxygen (O_2)
Al 6061-T6				
No Titanate	-730 mV	-700 mV	0.19 $\mu A/cm^2$	5.0 $\mu A/cm^2$
With Titanate – Al Rxn	-760 mV	-760 mV	0.94 $\mu A/cm^2$	1.7 $\mu A/cm^2$
With Titanate – Ti Rxn	-1.18 V	-1.16 V	0.94 $\mu A/cm^2$	1.7 $\mu A/cm^2$
Al 7075-T6				
No Titanate	-820 mV	-700 mV	1.0 $\mu A/cm^2$	20 $\mu A/cm^2$
With Titanate – Al Rxn	-740 mV	-760 mV	1.9 $\mu A/cm^2$	2.25 $\mu A/cm^2$
With Titanate – Ti Rxn	-1.15 V	-1.15 V	1.9 $\mu A/cm^2$	2.25 $\mu A/cm^2$

Table 4-1: Data for open circuit potentials (OCP) and current densities (*i*) for Al 6061-T6 and Al 7075-T6.

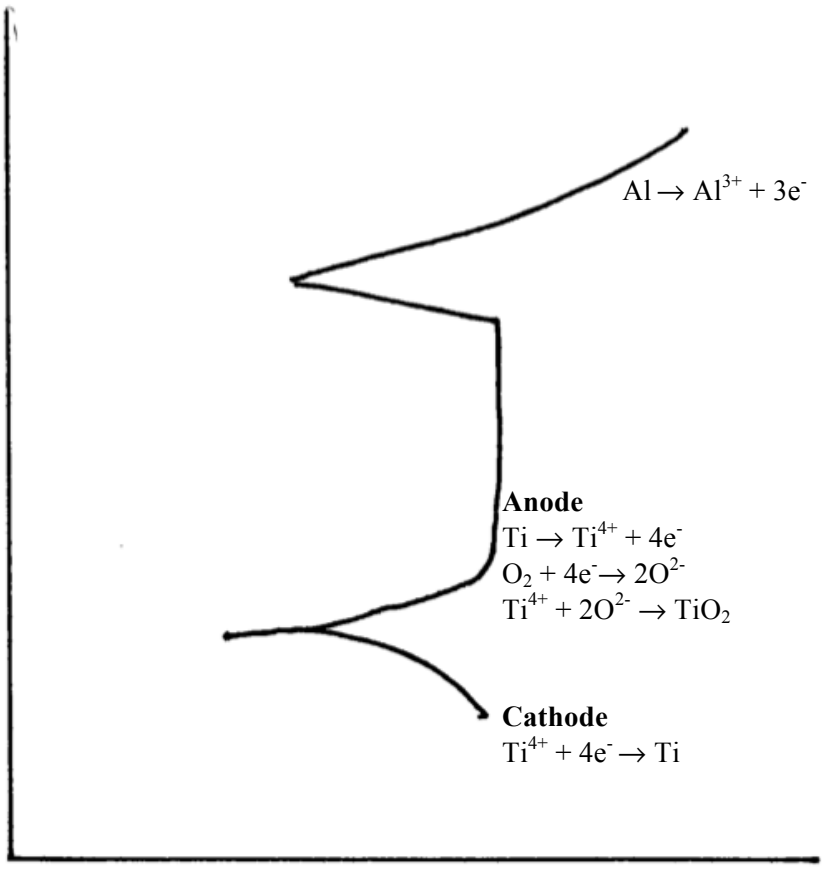

Figure 4-1: Cathodic and anodic reactions present in the potentiodynamic data.

a. single pit

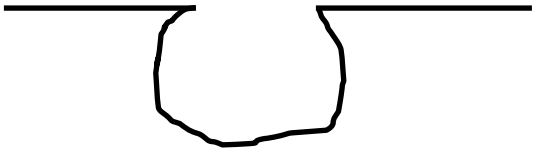

b. multiple pits

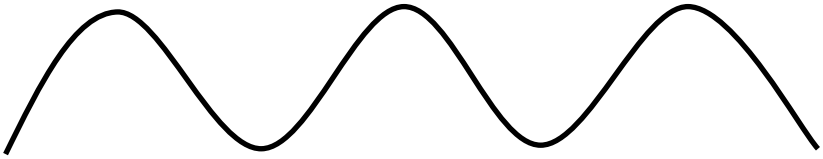

Figure 4-2: Mechanical explanations for coating failure.

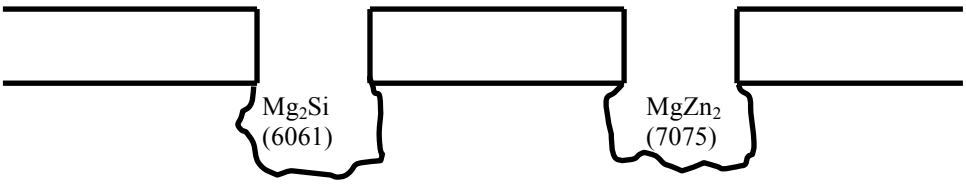

Figure 4-3: Microstructural explanations for poor coating performance.

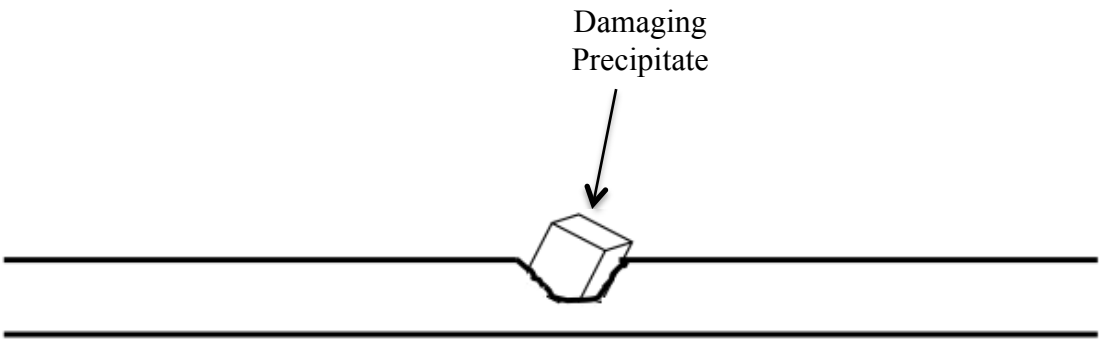

Figure 4-4: Coating failure due to chemical precipitates.

References

1. Brown, R. Chapter 5: Localized Corrosion. Retrieved from Lecture Online Web Site: http://www.egr.uri.edu/che/course/CHE534w/CHE534Index.htm, Feburary 10, 2011.

2. Rangel, C.M. and T.I.C. Paiva (1996). Chromium ion implantation for inhibition of corrosion of aluminium. *Surface & Coatings Technology*, 83(1-3): p. 194-200.

3. Grilli, R., et al. (2011). Corrosion behaviour of a 2219 aluminum alloy treated with a chromate conversion coating exposed to a 3.5% NaCl solution. *Corrosion Science*: p. doi:10.1016/j.corsci.2010.12.006.

4. Davis, J.R. (1999). Corrosion of Aluminum and Aluminum Alloys, ASM International, p. 35.

5. Maddala, D. (2007). An Alternate Coating Process for Corrosion Resistance on Aluminum Alloy 2024-T3. MS Thesis, University of Rhode Island.

6. Huang, H.H. (2002). Electrochemical impedance spectroscopy study of strained titanium in fluoride media. *Electrochimica Acta*, 47(13-14): p. 2311-2318.

7. Schiff, N., et al. (2002). Influence of fluoride content and pH on the corrosion resistance of titanium and its alloys. *Biomaterials*, 23(9): p. 1995-2002.

Chapter V

Recommendations and Future Research

A detailed study should be conducted to determine the optimum concentration of sodium fluoride (NaF) in the conversion coating bath. Titanate coating baths should be made with NaF concentrations of 0 g/L, 1 g/L and 2 g/L in order to determine the optimum concentration, in which fluoride precipitates will not be present on the surface.

The solubility limit of NaF in solution needs to be determined under conversion coating conditions.

In addition, research should be conducted to quantify the surface roughness of the alloys. This can be done by stereo imaging in scanning electron microscope images.

Thorough research also should be done to determine the concentration of Ti^{2+} and Ti^{4+} ions in the conversion coating bath. Also the solubility limit of titanate ions in the solution should be measured so the optimum amount of potassium titanium oxide is in the conversion coating solution, thus addition of excess amounts can be minimized to optimize the cost.

Further investigation is required to verify that the titanate ion protects aluminum alloys Al 6061-T6 and Al 7075-T6 against crevice corrosion.

BIBLIOGRAPHY

Brown, R. Chapter 1: Introduction. Retrieved from Lecture Online Web Site: http://www.egr.uri.edu/che/course/CHE534w/CHE534Index.htm, February 8, 2011.

Brown, R. Chapter 5: Localized Corrosion. Retrieved from Lecture Online Web Site: http://www.egr.uri.edu/che/course/CHE534w/CHE534Index.htm, February 10, 2011.

Buchheit, R.G. (1995). A Compilation of Corrosion Potentials Reported for Intermetallic Phases in Aluminum-Alloys. *Journal of the Electrochemical Society*, 142(11): p. 3994-3996.

Campestrini, P., et al. (2004). Chromate conversion coating on aluminum alloys - I. Formation mechanism. *Journal of the Electrochemical Society*, 151(2): p. B59- B70.

Chen, W.K., et al. (2010). The effect of chromic sulfate concentration and immersion time on the structures and anticorrosive performance of the Cr(III) conversion coatings on aluminum alloys. *Applied Surface Science*, 256(16): p. 4924-4929.

Cohen, S.M. (1995). Review - Replacements for Chromium Pretreatments on Aluminum. *Corrosion*, 51(1): p. 71-78.

Davis, J.R. (1999). Corrosion of Aluminum and Aluminum Alloys, ASM International, p. 30.

Davis, J.R. (1999). Corrosion of Aluminum and Aluminum Alloys, ASM International, p. 35.

Davis, J.R. (1999). Corrosion of Aluminum and Aluminum Alloys, ASM International, p. 206-208.

Davis, J.R. (1999). Corrosion of Aluminum and Aluminum Alloys, ASM International, p. 209.

Davis, J.R. (1999). Corrosion of Aluminum and Aluminum Alloys, ASM International, p. 267.

Dey, S., M.K. Gunjan, and I. Chattoraj (2008). Effect of temper on the distribution of pits in AA7075 alloys. *Corrosion Science*, 50(10): p. 2895-2901.

Ezuber, H., A. El-Houd, and F. El-Shawesh (2008). A study on the corrosion behavior of aluminum alloys in seawater. *Materials & Design*, 29(4): p. 801-805.

Grilli, R., et al. (2011). Corrosion behaviour of a 2219 aluminum alloy treated with a chromate conversion coating exposed to a 3.5% NaCl solution. *Corrosion Science*, 53(4): p. 1214-1223.

He, X.D. and X.M. Shi (2009). Self-repairing coating for corrosion protection of aluminum alloys. *Progress in Organic Coatings*, 65(1): p. 37-43.

Huang, H.H. (2002). Electrochemical impedance spectroscopy study of strained titanium in fluoride media. *Electrochimica Acta*, 47(13-14): p. 2311-2318.

Jayaganthan, R., et al. (2010). Microstructure and texture evolution in cryorolled Al 7075 alloy. *Journal of Alloys and Compounds*, 496(1-2): p. 183-188.

Jogi, B.F., et al. (2008). Some studies on fatigue crack growth rate of aluminum alloy 6061. *Journal of Materials Processing Technology*, 201(1-3): p. 380-384.

Kendig, M.W. and R.G. Buchheit (2003). Corrosion inhibition of aluminum and aluminum alloys by soluble chromates, chromate coatings, and chromate-free coatings. *Corrosion*, 59(5): p. 379-400.

Liu, Y., et al. (2005). Ageing effects in the growth of chromate conversion coatings on aluminium. *Corrosion Science*, 47(1): p. 145-150.

Lunder, O., et al. (2005). Formation and characterisation of a chromate conversion coating on AA6060 aluminium. *Corrosion Science*, 47(7): p. 1604-1624.

Lytle, F.W., et al. (1995). An Investigation of the Structure and Chemistry of a Chromium-Conversion Surface-Layer on Aluminum. *Corrosion Science*, 37(3): p. 349-369.

Maddala, D. (2007). An Alternate Coating Process for Corrosion Resistance on Aluminum Alloy 2024-T3. MS Thesis, University of Rhode Island.

Maddala, D. (2007). An Alternate Coating Process for Corrosion Resistance on Aluminum Alloy 2024-T3. MS Thesis, University of Rhode Island, p. 4.

Niknahad, M., S. Moradian, and S.M. Mirabedini (2010). The adhesion properties and corrosion performance of differently pretreated epoxy coatings on an aluminium alloy. *Corrosion Science*, 52(6): p. 1948-1957.

OSHA. "Hexavalent Chromium", Occupational Safety and Health Administration, 2009.

Pourbaix, M. (1966). Atlas of electrochemical equilibria in aqueous solutions, Pergamon Press, p. 215.

Rangel, C.M. and T.I.C. Paiva (1996). Chromium ion implantation for inhibition of corrosion of aluminium. *Surface & Coatings Technology*, 83(1-3): p. 194-200.

Scamans, G.M., N. Birbilis, and R.G. Buchheit (2010). Shreir's Corrosion: Corrosion of Aluminum and its Alloys, p. 1986-1987.

Scamans, G.M., N. Birbilis, and R.G. Buchheit (2010). Shreir's Corrosion: Corrosion of Aluminum and its Alloys, p. 2002-2003.

Scamans, G.M., N. Birbilis, and R.G. Buchheit (2010). Shreir's Corrosion: Corrosion of Aluminum and its Alloys, p. 2003.

Scamans, G.M., N. Birbilis, and R.G. Buchheit (2010). Shreir's Corrosion: Corrosion of Aluminum and its Alloys, p. 2005.

Schiff, N., et al. (2002). Influence of fluoride content and pH on the corrosion resistance of titanium and its alloys. *Biomaterials*, 23(9): p. 1995-2002.

Tucker, W.C. (2006). A non chromate conversion coating process for corrosion protection of AL2024 aluminum alloys in marine environment. *RINA Conference on Advanced Marine Materials & Coatings*: p. 71-75.

Wranglen, G. (1984). An Introduction to Corrosion and Protection of Metals, Chapman and Hall Ltd, p. 251-252.

Xia, L., et al. (2000). Storage and release of soluble hexavalent chromium from chromate conversion coatings - Equilibrium aspects of Cr-VI concentration. *Journal of the Electrochemical Society*, 147(7): p. 2556-2562.

Young, J.J. "Memorandum for Secretaries of the Military Departments: Minimizing the Use of Hexavalent Chromium (Cr6+)", Department of Defense, April 8, 2009.